

# Modeling the Vapor-Liquid Equilibria of Sustainable Aviation Fuel Components with Nitrogen Using the PC-SAFT Equation of State

Aaron J. Rowane,<sup>\*,†</sup> Davide Menegazzo,<sup>‡</sup> and Ian H. Bell<sup>†</sup>

<sup>†</sup>*Applied Chemicals and Materials Division, National Institute of Standards and Technology, Boulder, CO 80305*

<sup>‡</sup>*Department of Industrial Engineering–Applied Physics Section, University of Padova, 35131 Padova, Italy and Construction Technologies Institute, National Research Council (ITC-CNR), 35127 Padova, Italy.*

E-mail: aaron.rowane@nist.gov

## Abstract

The vapor-liquid equilibrium (VLE) of fuel-N<sub>2</sub> mixtures are modeled using the perturbed-chain statistical associating fluid theory (PC-SAFT) equation of state (EoS), where in this study “fuel” refers to a pure component hydrocarbon. These mixtures are important in evaluating the thermodynamic state of the fuel-air mixture in the combustion chamber where N<sub>2</sub> serves as a surrogate for air. NIST ThermoDataEngine (TDE) was used to catalog fuel-N<sub>2</sub> data sets for fuel components expected in sustainable aviation fuels. The goal of this study was to develop a predictive model capable of capturing the structure-property relationships of fuel components in the presence of N<sub>2</sub>. Therefore, PC-SAFT model parameters were estimated using a group contribution method, which consider the fuel’s molecular structure. Binary interaction parameters ( $k_{ij}$ ) were fit for each fuel-N<sub>2</sub> mixture data set and a correlation for  $k_{ij}$  values for fuel-N<sub>2</sub> mixtures was derived. PC-SAFT calculations using fitted parameters reproduced most of the experimental data within an average mole fraction residual of 0.04 and 0.08 for the liquid and vapor phases, respectively. VLE calculations using fitted and correlated  $k_{ij}$  values yielded similar

performance for most fuel-N<sub>2</sub> binary mixtures.

## 1 Introduction

Data from the Bureau of Transportation Statistics shows that in 2023 the consumption of aviation fuel by all major airline carriers exceeded 12.9 billion gallons (48,832 cubic meters), which is 9.4% greater than that in 2022.<sup>1</sup> The aviation industry is currently responsible for roughly 2% of global carbon emissions and the demand for air transport is expected to increase. The Biden administration proposed the Sustainable Aviation Fuel (SAF) Grand Challenge which aims to increase SAF production levels to three billion gallons annually by 2030. These three billion gallons of domestically produced SAF are expected to have 50% lower life-cycle greenhouse gas emissions than an equivalent amount of petroleum derived aviation fuel. The ultimate goal of the SAF grand challenge is to decarbonize the aviation industry by 2050<sup>2</sup> by increasing SAF production levels to 35 billion gallons (132,489 cubic meters) annually. Electrification of commercial aviation for high-capacity, long-haul flights is infeasible due to the high energy density requirements. Therefore, sustainable aviation fuels (SAF) with a carbon net-zero life cycle have been proposed.

SAF are a renewable and low-carbon alternative to petroleum-derived jet fuels produced from seven pathways certified by the American Society for Testing and Materials (ASTM).<sup>3</sup> These pathways are: Fisher-Tropsch (FT) synthesis, Hydrotreated Esters and Fatty Acids (HEFA), Synthesized Iso-paraffinic (SIP), Alcohol to Jet (ATJ), Fats, Oils, and Greases (FOG) Co-processing, Catalytic Hydrothermolysis (CH), and FT Co-processing. Collectively, the feed stocks for these processes include biomass, waste oil, hydrogen, and alcohols. The products from all of these processes are compounds found in petroleum derived fuels, which include *n*-paraffins, *i*-paraffins, naphthenes, and for certain processes aromatics.<sup>4</sup> Despite the compositional similarities of SAF to traditional jet fuels, presently SAF produced from all pathways, must still be used in blends with conventional petroleum based jet fuel to ensure a balanced composition of paraffins, olefins, and aromatics. SAF produced from FT, HEFA, SIP, ATJ can all be blended at ratios up to 50% with conventional jet fuel to produce a finished fuel. However, fuels produced from the FOG and FT co-processing pathways can only be blended at the 5% level. While it would be desirable to completely eliminate aromatic compounds from SAF due to their poor combustion characteristics, they are required in certain amounts to promote o-ring swelling<sup>5</sup> to ensure proper sealing of aircraft engine components. It is important to note that out of the approved SAF pathways CH is the only one that produces aromatic compounds in significant amounts.<sup>4</sup>

The chemical structure of the components found in SAF govern the thermophysical properties of the fuel. Thermophysical property differences between structural isomers can become more pronounced at the high-pressure, high-temperature conditions (HPHT) encountered in jet engines. To advance the design of aircraft engines and further increase their efficiency, knowledge of the fuel’s thermophysical properties and thermodynamic state is critical. The range of conditions that the fuel exhibits when it encounters air in the aircraft combustor is broad. Colket et al.<sup>6</sup> show that at high altitude the combustion chamber inlet temper-

atures can approach 200 K at corresponding chamber pressures of less than 0.1 MPa. Colket et al.<sup>6</sup> also show that under normal operating conditions the combustion chamber pressures and temperatures can reach temperatures of 800 K and pressures of 2.5 MPa. During take off when significant thrust is required the combustor pressure can be as high as 8 MPa. As highlighted in the literature,<sup>7,8</sup> future aircraft engine design may push operating combustor pressures higher, which would enable supercritical combustion offering diffuse mixing of the fuel with air. Several novel compounds have been identified within sustainable aviation fuels, which in some cases include strained-rings,<sup>2</sup> that are expected to be unstable at HPHT conditions. Therefore, thermophysical property measurements and modeling at high pressures and temperatures may be challenging.

The focus of this study is to propose a modeling technique to determine the thermodynamic state of the fuel in the presence of air that can capture the impact of chemical structure and be extrapolated to determine the properties of compounds that are challenging to measure accurately. Fuel-nitrogen( $N_2$ ) mixtures are typically studied to simulate the phase behavior of fuel-air mixtures while avoiding potential combustion reactions with oxygen at HPHT conditions. Therefore, due to the lack of fuel-air phase behavior data, in this work  $N_2$  serves as an inert surrogate for air to simulate VLE of the fuel-air mixture.

While REFPROP (version 10.0)<sup>9</sup> includes several Helmholtz-energy-explicit EoS for fluids present in SAF which can be used to model mixtures with the multifluid model,<sup>10</sup> the algorithms present in REFPROP are not optimized to handle highly asymmetric mixtures (i.e., mixtures with large differences in molar mass or volatility) of SAF constituents with nitrogen. In this study, the Templated Equation of state Package (teqp) is used to model fuel- $N_2$  mixtures. teqp utilizes automatic differentiation rather than analytical derivatives to calculate thermodynamic properties. This approach is more agile, allowing for the quicker implementation of EoS since it eliminates the need for human-derived, hand-written deriva-

tives. Further, the use of automatic differentiation does not impose any computational cost penalties relative to calculations performed using analytical derivatives. The current version of `teqp` implements several equations of state (EoS) including cubic EoS, the perturbed-chain statistical associating fluid theory EoS (PC-SAFT EOS),<sup>11</sup> and Helmholtz-energy explicit EoS.

The Helmholtz-energy-explicit EoS is completely empirical and can have a hundred or more adjustable parameters, which are obtained from a simultaneous fit of several thermodynamic properties including the vapor pressure, vapor and liquid densities, speed of sound, and heat capacity. The Helmholtz-energy-explicit EoS can provide reference quality thermodynamic property values when fit to reference quality data. However, the predictive capabilities of empirical EoS are limited since Helmholtz-energy Explicit EoS parameters are specific to a single molecule. The predictive capabilities of the Helmholtz-energy-explicit EoS are extrapolations at conditions beyond those for which experimental data were fit and for mixtures using estimated binary interaction parameters as described by Bell and Lemmon.<sup>12</sup> However, it needs to be restated that predictions for binary mixtures are still contingent on the availability of fluid-specific pure fluid equations of state for each mixture component. It is also important to note that while the fitting procedure for Helmholtz-energy-explicit EoS has evolved, not all of these EoS are created equal. Careful attention has been paid to model extrapolations to ensure the calculations do not provide non-physical behavior, which can lead to further errors when included in a multifluid model. Deiters and Bell<sup>13</sup> identified non-physical behavior in the mixture critical curves calculated using several multifluid models for binary mixtures in which an unreasonable temperature maxima was observed above the fuel component’s critical point. Deiters and Bell attributed this non-physical behavior to faulty pure fluid Helmholtz-Energy-Explicit EoS. Presently, the scope of the fluid-specific EoS presently available in REFPROP is not only insufficient to propose surrogate mod-

els for fuel-N<sub>2</sub> mixtures, but non-physical behavior occurs at conditions leading up to combustion.

Both cubic and PC-SAFT EoS are semi-empirical and only require limited experimental data to obtain model parameters. The inputs for cubic EoS are the critical temperature, critical pressure, and acentric factor (obtained from a fit of the vapor pressure curve) for the fluid of interest. The PC-SAFT EoS has three parameters related to the molecular structure of a fluid which are usually obtained from a fit of the vapor pressure curve and the coexisting vapor and liquid densities. Several group contribution (GC) methods are available to estimate PC-SAFT EoS parameters. The flexibility of both cubic and PC-SAFT EoS comes at the expense of being incapable of reproducing experimentally determined thermodynamic properties within their specified uncertainties. However, both cubic and the PC-SAFT EoS are generally well behaved and typically do not produce non-physical behavior. The PC-SAFT EoS generally provides a better description of thermodynamic properties than cubic EoS. Therefore, the PC-SAFT EoS was selected for this work. Group contribution methods were used to estimate model PC-SAFT model parameters based on their chemical structure, and binary interaction parameters were fit to the available literature data. A correlation for  $k_{ij}$  values for fuel-N<sub>2</sub> mixtures was developed. This allows for a purely predictive methodology for fuel-N<sub>2</sub> mixture phase behavior.

## 2 Methods

In the following section all of the vapor-liquid equilibrium data for petroleum fuel-N<sub>2</sub> mixtures are catalogued and the PC-SAFT EoS is introduced with code that can be used to trace an isotherm. Table 1 lists the fuels investigated in this study with the REFPROP name, CAS number, critical temperature, critical pressure, and molecular mass. The REFPROP fluid name is used in figures and tables throughout this study as they are more concise.

Table 1: Fluids investigated in this study. Listed are the full fluid name, REFPROP Name, CAS number, critical temperature ( $T_c$ ), critical pressure ( $p_c$ ), and molecular weight ( $MW$ ).

Fluid	REFPROP Name	CAS	$T_c$ / K	$p_c$ / MPa	$MW$ / g·mol <sup>-1</sup>
methane	METHANE	74-82-8	190.56	4.595	16.04
ethane	ETHANE	74-84-0	305.32	4.872	30.07
propane	PROPANE	74-98-6	369.89	4.251	44.10
butane	BUTANE	106-97-8	425.13	3.796	58.12
pentane	PENTANE	109-66-0	469.70	3.368	72.15
hexane	HEXANE	110-54-3	507.82	3.044	86.18
heptane	HEPTANE	142-82-5	540.20	2.736	100.20
octane	OCTANE	111-65-9	598.74	2.484	114.23
nonane	NONANE	111-84-2	594.55	2.281	128.26
decane	DECANE	124-18-5	617.70	2.103	142.28
undecane	C11	1120-21-4	638.80	1.990	156.31
dodecane	C12	112-40-3	658.10	1.817	170.33
hexadecane	C16	544-76-3	722.10	1.480	226.45
eicosane	C20	112-95-8	771.38	1.198	282.55
octacosane	C28	630-02-4	827.40	0.661	394.76
hexatriacontane	C36	630-06-8	864.00	0.428	506.97
isobutane	ISOBUTAN	75-28-5	407.81	3.629	58.12
2-methylbutane	IPENTANE	78-78-4	460.35	3.378	72.15
2,2-dimethylpropane	NEOPENTN	463-82-1	433.74	3.196	72.15
2,2,4-trimethylpentane	IOCTANE	540-84-1	544.00	2.572	114.23
2,2,4,4,6,8,8-heptamethylnonane	ISOC16	4390-04-9	691.90	1.527	226.44
cyclopentane	CYCLOPEN	287-92-3	511.72	4.583	70.13
cyclohexane	CYCLOHEX	110-82-7	553.60	4.081	84.16
methylcyclohexane	C1CC6	108-87-2	572.20	3.470	98.19
propylcyclohexane	C3CC6	1678-92-8	630.80	2.860	126.24
JP-10	JP-10	2825-82-3	698.00	3.733	136.23
<i>trans</i> -decalin	TDEC	493-02-7	687.02	3.128	138.25
cyclododecane	CYCLODODEC	294-62-2	764.23	2.546	168.32
benzene	BENZENE	71-43-2	562.02	4.907	78.11
methylbenzene	TOLUENE	108-88-3	591.75	4.126	92.14
1,4-dimethylbenzene	PXYLENE	106-42-3	616.17	3.515	106.17
1,2,3-trimethylbenzene	124MBEN	95-63-6	649.12	3.289	120.19
1,3,5-trimethylbenzene	135MBEN	108-67-8	639.00	3.160	120.19
propylbenzene	C3BEN	103-65-1	638.40	3.200	120.19
1,3-dimethylbenzene	MXYLENE	108-38-3	616.89	3.535	106.17
1-methylnaphthalene	1MNAPHTH	90-12-0	770.70	3.559	142.20
naphthalene	NAPHTH	91-20-3	748.00	4.100	128.17
phenanthrene	PHENANTH	85-01-8	873.20	3.300	178.23
pyrene	PYRENE	129-00-0	938.20	2.600	202.25
1,2,3,4-tetrahydronaphthalene	TETRALIN	119-64-2	720.10	3.579	132.20

## 2.1 Review of Available Literature Data

Table 2 lists available fuel-N<sub>2</sub> literature data obtained from NIST ThermoDataEngine (TDE). Listed for each study is the REFPROP name, citation for each study, temperature and pressure ranges studied, vapor and liquid composition space covered, and the total number of data points reported. Fig. 1 provides a condensed visual representation of the available vapor-liquid equilibrium data listed in Table 2 for fuel-N<sub>2</sub> mixtures. In Fig. 1 compounds are organized by chemical family and then by increasing molar mass. Different studies are represented by the colored boxes shown in each bar. In total 7433 data points from 117 unique studies were used to develop and evaluate the model in this study. Fig. 1 shows that with increasing molar mass and molecular complexity the number of data sets available in the literature decreases. While olefins are a chemical family found in fuels, the available data for olefin-nitrogen mixtures are extremely limited and were excluded from this study.

Fig. 2 represents the available literature data that are most relevant to compounds expected in SAF. Certified SAFs are required to have properties and compositions similar to that of traditional jet fuels. Typically, the average carbon number of jet fuels is twelve with the mixture components ranging from seven to eighteen carbons<sup>6</sup>. As discussed in the introduction, pressures expected in the combustor are less than 8 MPa with temperature ranging from 200 K to 800 K. Therefore, what is shown in Fig. 2 are fuels that have carbon numbers ranging from seven to seventeen and data points limited to pressures of 8 MPa. The total number of data points remaining in Fig. 2 is 795 from 67 independent studies, which is just over 10% of the data included in this study. However, as will be shown in preceding sections, all of the data shown in Fig. 1 and listed in Table 2 are useful for model development.

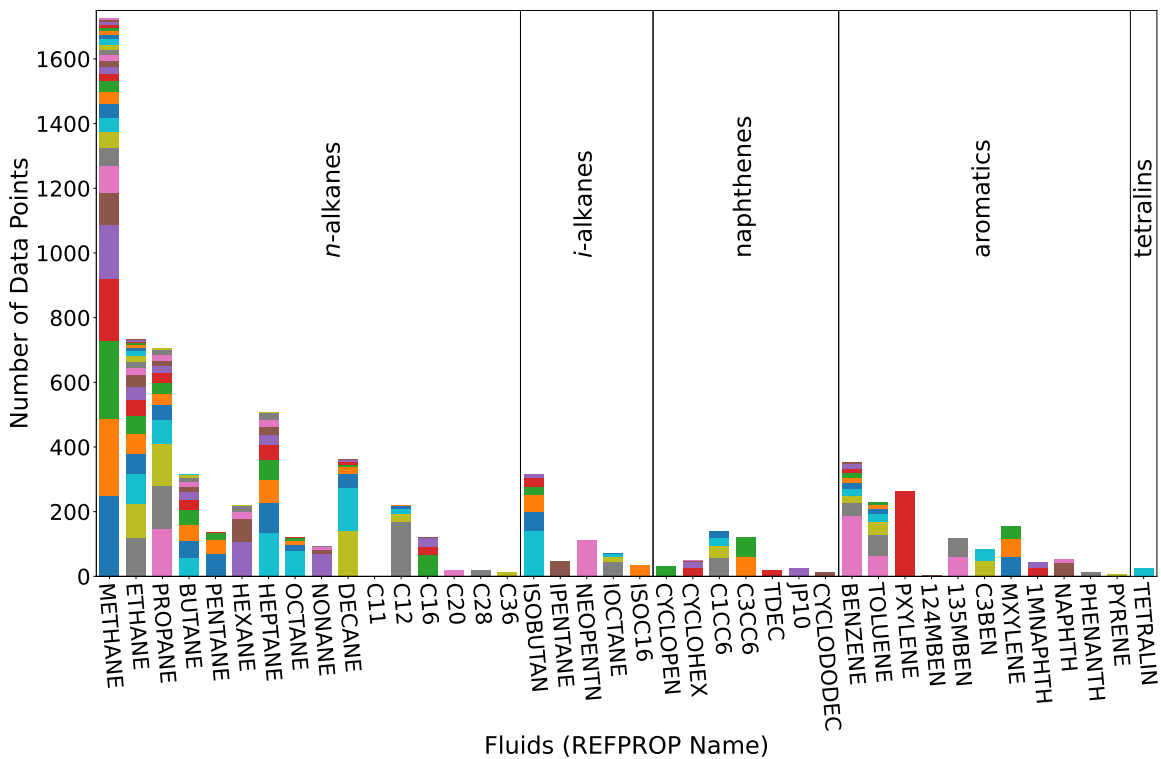


Figure 1: Available fuel-N<sub>2</sub> vapor-liquid equilibrium literature data obtained from NIST ThermoDataEngine. Components are sorted by chemical family and then molar mass. Different colors in each bar represent a separate study.

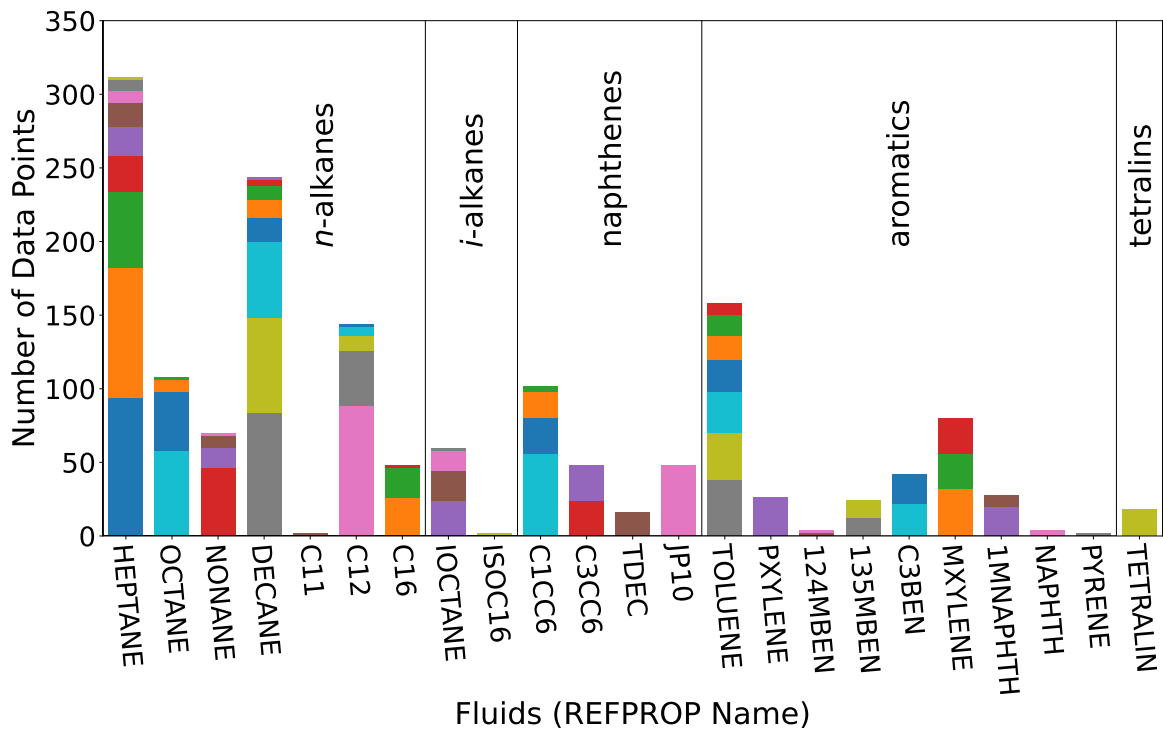


Figure 2: Available fuel-N<sub>2</sub> vapor-liquid equilibrium literature data obtained from NIST ThermoDataEngine for fuel components most relevant to SAF. Data were filtered down to only include data points for compounds with carbon numbers ranging from seven to eighteen and at pressures below 10 MPa. Different colors in each bar represent a separate study.

Table 2: Available fuel-N<sub>2</sub> vapor-liquid equilibrium literature data obtained from NIST Thermo-DataEngine. Listed for each study are the temperature range ( $T_{\text{range}}$ ), pressure range ( $p_{\text{range}}$ ), liquid ( $x_{\text{N}_2,\text{range}}$ ) and vapor ( $y_{\text{N}_2,\text{range}}$ ) molar composition, and number of data points available ( $n$ ).

Fluid	Study	$T_{\text{range}} / \text{K}$	$p_{\text{range}} / \text{MPa}$	$x_{\text{N}_2,\text{range}}$	$y_{\text{N}_2,\text{range}}$	$n$
<i>n</i> -alkanes						
METHANE	McTaggart and Edwards <sup>14</sup>	84-106	0.1	0.03-0.54	0.08-0.77	7
METHANE	Torocheshnikov and Levius <sup>15</sup>	90-133	0.1-2.3	0.02-0.78	0.15-0.98	44
METHANE	Bloomer and Parent <sup>16</sup>	91-190	0.1-5.1	0.01-0.95	0.01-0.95	240
METHANE	Cines et al. <sup>17</sup>	100-172	0.1-4.5	0.01-0.99	0.04-0.99	192
METHANE	Fastovskii and Petrovskii <sup>18</sup>	82-157	0.1-1.6	0.01-0.90	0.06-0.99	228
METHANE	Brandt and Stroud <sup>19</sup>	137-175	3.4	0.05-0.71	0.13-0.84	18
METHANE	Cheung and Wang <sup>20</sup>	92-124	<0.1-0.6	0.01-0.15	0.10-0.86	40
METHANE	Sprow and Prausnitz <sup>21</sup>	91	0.1-0.4	0.13-0.95	0.89-0.99	18
METHANE	Chang and Lu <sup>22</sup>	122-171	0.3-5.0	0.02-0.99	0.05-0.99	53
METHANE	Fuks and Bellemans <sup>23</sup>	84-91	0.1-0.2	0.14-0.67	-	20
METHANE	Skripka et al. <sup>24</sup>	113	0.1-1.6	0.05-0.95	0.05-0.95	12
METHANE	Miller et al. <sup>25</sup>	112	0.2-1.3	0.03-0.78	-	11
METHANE	Stryjek et al. <sup>26</sup>	114-183	0.2-5.0	<0.01-0.99	0.01-0.99	214
METHANE	Kidnay et al. <sup>27</sup>	112-180	0.2-4.9	<0.01-0.90	0.02-0.94	166
METHANE	Wilson <sup>28</sup>	111	0.2-1.3	0.06-0.86	-	14
METHANE	McClure et al. <sup>29</sup>	91	0.1-0.3	0.19-0.88	0.92-0.99	16
METHANE	Hiza et al. <sup>30</sup>	95-140	0.1-2.1	0.05-0.49	-	21
METHANE	Kremer <sup>31</sup>	140-160	0.7-4.9	<0.01-0.79	0.02-0.82	32
METHANE	Kremer and Knapp <sup>32</sup>	120-144	1.5-4.0	0.27-0.73	0.38-0.90	15
METHANE	Llave et al. <sup>33</sup>	118-138	1.9-3.7	0.69-0.95	-	4
METHANE	Liu et al. <sup>34</sup>	123	0.4-2.6	0.05-0.91	0.43-0.97	10
METHANE	Rozhnov et al. <sup>35</sup>	133-180	0.7-4.4	-	0.07-0.40	49
METHANE	Jin et al. <sup>36</sup>	123	0.4-2.6	0.05-0.91	0.43-0.97	10
METHANE	Parrish and Hiza <sup>37</sup>	95-115	0.2-1.7	0.13-0.90	0.78-0.98	80
METHANE	Janisch et al. <sup>38</sup>	130-180	0.6-5.1	0.02-0.59	0.09-0.70	35
METHANE	Han et al. <sup>39</sup>	100-123	<0.1-1.3	<0.01-0.86	0.13-0.99	70
ETHANE	Ellington et al. <sup>40</sup>	101-298	0.7-10.0	0.05-0.98	-	95
ETHANE	Cheung and Wang <sup>20</sup>	93	<0.1	0.99	-	2
ETHANE	Chang and Lu <sup>22</sup>	122-171	0.3-3.4	0.03-0.97	0.56-0.99	43
ETHANE	Stryjek et al. <sup>41</sup>	139-194	0.3-13.5	0.01-0.73	0.49-0.99	96
ETHANE	Wilson <sup>28</sup>	111	0.2-1.5	0.02-0.99	-	13
ETHANE	Grauso et al. <sup>42</sup>	200-290	0.7-13.2	0.01-0.57	0.10-0.91	31
ETHANE	Hiza et al. <sup>30</sup>	105-120	0.4-0.6	0.06	-	4
ETHANE	Gupta et al. <sup>43</sup>	260-280	1.8-9.9	<0.01-0.37	0.04-0.57	113
ETHANE	Kremer <sup>31</sup>	120-133	0.6-3.6	0.04-0.99	0.99	21
ETHANE	Kremer and Knapp <sup>44</sup>	120-133	0.6-4.1	0.04-0.99	0.99	58
ETHANE	Zeck and Knapp <sup>45</sup>	240-260	1.9-7.5	0.02-0.20	0.24-0.72	15
ETHANE	Rozhnov et al. <sup>35</sup>	177-281	0.5-7.2	-	0.14-0.82	59
ETHANE	Brown et al. <sup>46</sup>	220-270	0.8-12.0	0.01-0.82	0.22-0.83	59
ETHANE	Zhang et al. <sup>47</sup>	233-253	3.0-4.0	0.06-0.08	0.52-0.66	4

Continued on next page

Table 2: Available fuel-N<sub>2</sub> vapor-liquid equilibrium literature data obtained from NIST Thermo-DataEngine. Listed with each study are the temperature range ( $T_{\text{range}}$ ), pressure range ( $p_{\text{range}}$ ), liquid ( $x_{\text{N}_2,\text{range}}$ ) and vapor ( $y_{\text{N}_2,\text{range}}$ ) molar composition, and number of data points available ( $n$ ).

Fluid	Study	$T_{\text{range}} / \text{K}$	$p_{\text{range}} / \text{MPa}$	$x_{\text{N}_2,\text{range}}$	$y_{\text{N}_2,\text{range}}$	$n$
ETHANE	Raabe et al. <sup>48</sup>	210-270	1.1-10.0	0.02-0.33	0.23-0.86	11
ETHANE	Guedes and Zollweg <sup>49</sup>	91	0.1-0.4	0.01-0.99	-	7
ETHANE	Raabe and Kohler <sup>50</sup>	120-138	0.9-3.3	0.05-0.27	0.99	21
ETHANE	Janisch et al. <sup>38</sup>	150-270	0.6-10.1	0.02-0.36	0.23-0.99	36
PROPANE	Bolshakov and Linshits <sup>51</sup>	298	2.5-18.1	0.03-0.55	0.55-0.78	16
PROPANE	Cheung and Wang <sup>20</sup>	92-128	0.1-0.6	0.01-0.07	0.99	13
PROPANE	Schindler et al. <sup>52</sup>	143-353	1.4-13.8	0.01-0.32	0.14-0.99	114
PROPANE	Cannon et al. <sup>53</sup>	172-256	2.1-4.8	0.03-0.11	-	32
PROPANE	Yorizane et al. <sup>54</sup>	195-296	0.5-6.3	0.01-0.09	0.23-0.99	19
PROPANE	Grauso et al. <sup>42</sup>	230-290	1.2-21.9	0.02-0.53	0.54-0.96	32
PROPANE	Hiza et al. <sup>30</sup>	100-115	0.4-0.9	0.02-0.07	-	6
PROPANE	Kremer <sup>31</sup>	120-127	0.7-6.2	0.03-0.13	0.99	17
PROPANE	Kremer and Knapp <sup>44</sup>	120-127	0.7-6.2	0.03-0.99	0.99	45
PROPANE	Hudziak et al. <sup>55</sup>	188-343	0.1-5.8	-	0.26-0.91	127
PROPANE	Rozhnov et al. <sup>35</sup>	196-285	0.1-4.8	-	0.18-0.89	147
PROPANE	Poon and Lu <sup>56</sup>	114-122	0.2-2.5	0.01-0.09	0.99	25
PROPANE	Yucelen and Kidnay <sup>57</sup>	240-330	1.2-15.1	0.02-0.32	0.23-0.95	71
BUTANE	Sauer <sup>58</sup>	311-378	0.7-20.7	<0.01-0.44	0.39-0.89	11
BUTANE	Roberts and McKetta <sup>59</sup>	311-411	1.6-23.5	0.03-0.49	0.14-0.90	58
BUTANE	Roberts and McKetta <sup>60</sup>	378	3.4	0.05	0.40	2
BUTANE	Lehigh and McKetta <sup>61</sup>	311	13.9-28.8	0.23-0.63	0.63-0.90	14
BUTANE	Steinbach and Steinbrecher <sup>62</sup>	273-293	0.4-1.1	0.01-0.03	-	12
BUTANE	Hudziak et al. <sup>55</sup>	240-310	0.2-6.9	-	0.87-0.95	50
BUTANE	Brown et al. <sup>63</sup>	250-344	0.5-15.8	<0.01-0.27	0.18-0.98	50
BUTANE	Malewski and Sandler <sup>64</sup>	339-380	1.2-22.1	0.02-0.51	0.19-0.83	30
BUTANE	Shibata and Sandler <sup>65</sup>	311-411	1.1-28.5	0.01-0.61	0.06-0.90	21
BUTANE	Brown et al. <sup>66</sup>	250-270	1.5-14.0	0.02-0.21	0.93-0.98	18
PENTANE	Kurata and Swift <sup>67</sup>	144-255	2.4-31.1	0.05-0.39	0.98-0.99	22
PENTANE	Preston and Prausnitz <sup>68</sup>	91-97	0.1	0.99	-	2
PENTANE	Kalra et al. <sup>69</sup>	277-378	0.3-20.8	<0.01-0.40	0.18-0.99	42
PENTANE	Silva-Oliver et al. <sup>70</sup>	344-448	1.7-35.5	0.01-0.63	0.10-0.94	71
HEXANE	Poston and McKetta <sup>71</sup>	311-444	1.7-34.5	0.02-0.70	0.57-0.99	106
HEXANE	Baranovich and Smirnova <sup>72</sup>	233-293	0.2-0.7	0.17-0.93	-	19
HEXANE	Hesse et al. <sup>73</sup>	298	0.1	0.01	-	1
HEXANE	Eliosa-Jimenez et al. <sup>74</sup>	345-488	1.0-51.5	0.01-0.67	0.13-0.97	72
HEXANE	Jabloniec et al. <sup>75</sup>	304-393	<0.1-3.4	<0.01-0.05	-	20
HEPTANE	Akers et al. <sup>76</sup>	305-455	7.0-69.1	0.08-0.75	0.83-0.99	71
HEPTANE	Peter and Eicke <sup>77</sup>	376-453	2.0-61.3	0.03-0.78	0.67-0.98	46
HEPTANE	Brunner et al. <sup>78</sup>	453-497	4.4-27.8	0.07-0.59	0.60-0.91	21
HEPTANE	Figuere et al. <sup>79</sup>	453-497	1.2-29.4	0.01-0.67	0.17-0.88	92
HEPTANE	Legret et al. <sup>80</sup>	305	9.1-99.8	0.11-0.66	0.94-0.99	62
HEPTANE	Llave and Chung <sup>81</sup>	305-366	5.5-34.9	0.06-0.40	-	22

Continued on next page

Table 2: Available fuel-N<sub>2</sub> vapor-liquid equilibrium literature data obtained from NIST Thermo-DataEngine. Listed with each study are the temperature range ( $T_{\text{range}}$ ), pressure range ( $p_{\text{range}}$ ), liquid ( $x_{\text{N}_2,\text{range}}$ ) and vapor ( $y_{\text{N}_2,\text{range}}$ ) molar composition, and number of data points available ( $n$ ).

Fluid	Study	$T_{\text{range}} / \text{K}$	$p_{\text{range}} / \text{MPa}$	$x_{\text{N}_2,\text{range}}$	$y_{\text{N}_2,\text{range}}$	$n$
HEPTANE	Waeterling et al. <sup>82</sup>	453	1.5-27.7	0.02-0.58	0.51-0.90	24
HEPTANE	Schlichting et al. <sup>83</sup>	252-273	1.5-9.3	-	0.99	32
HEPTANE	Hesse et al. <sup>73</sup>	298	0.1	<0.01	-	1
HEPTANE	Garcia-Sanchez et al. <sup>84</sup>	314-524	2.0-50.2	0.02-0.70	0.12-0.99	136
OCTANE	Baranovich and Smirnova <sup>72</sup>	233-293	0.2-0.7	0.11-0.79	-	20
OCTANE	Llave and Chung <sup>81</sup>	322-344	3.2-35.0	0.04-0.35	-	12
OCTANE	Daridon et al. <sup>85</sup>	293-373	15.8-21.2	0.21	-	9
OCTANE	Hesse et al. <sup>73</sup>	298	0.1	<0.01	-	1
OCTANE	Eliosa-Jimenez et al. <sup>86</sup>	344-544	2.0-50.1	0.02-0.70	0.18-0.99	73
NONANE	Llave and Chung <sup>81</sup>	322-344	3.7-34.7	0.05-0.33	-	12
NONANE	Schlichting et al. <sup>83</sup>	262-273	1.6-9.0	-	0.99	11
NONANE	Hesse et al. <sup>73</sup>	298	0.1	<0.01	-	1
NONANE	Silva-Oliver et al. <sup>87</sup>	344-543	2.0-49.8	0.03-0.67	0.36-0.99	70
DECANE	Prausnitz and Benson <sup>88</sup>	323-348	2.7-8.9	-	0.99	7
DECANE	Azarnoosh and McKetta <sup>89</sup>	311-411	1.7-34.5	<0.01-0.40	0.81-0.99	107
DECANE	D'Avila et al. <sup>90</sup>	323-398	3.2-10.2	-	0.99	9
DECANE	Llave and Chung <sup>81</sup>	344	4.0-34.6	0.07-0.38	-	6
DECANE	Pearce et al. <sup>91</sup>	263-311	0.2-20.1	-	0.99	44
DECANE	Hesse et al. <sup>73</sup>	298	0.1	<0.01	-	1
DECANE	Tong et al. <sup>92</sup>	344-411	3.9-16.0	0.06-0.20	-	21
DECANE	Garcia-Sanchez et al. <sup>93</sup>	345-563	1.0-50.3	0.02-0.71	0.35-0.99	142
C11	Hesse et al. <sup>73</sup>	298	0.1	<0.01	-	1
C12	D'Avila et al. <sup>90</sup>	348-423	7.1-9.4	-	0.99	9
C12	Llave and Chung <sup>81</sup>	328-366	3.1-34.7	0.05-0.35	-	16
C12	Hesse et al. <sup>73</sup>	298	0.1	<0.01	-	1
C12	Gao et al. <sup>94</sup>	344-411	1.3-9.6	0.02-0.13	-	24
C12	Garcia-Cordova et al. <sup>95</sup>	344-594	0.6-60.1	<0.01-0.77	0.17-0.99	169
C16	Sultanov et al. <sup>96</sup>	323-623	4.9-58.8	0.07-0.85	0.85-0.99	66
C16	Lin et al. <sup>97</sup>	463-703	2.0-25.5	0.04-0.56	0.26-0.99	27
C16	Hesse et al. <sup>73</sup>	298	0.1	<0.01	-	1
C16	Rowane et al. <sup>98</sup>	323-536	10.9-127.6	0.21-0.90	-	26
C20	Tong et al. <sup>92</sup>	323-423	3.8-17.2	0.06-0.21	-	20
C28	Tong et al. <sup>92</sup>	348-423	4.3-16.5	0.07-0.26	-	19
C36	Tong et al. <sup>92</sup>	373-423	5.3-18.0	0.11-0.30	-	12
<i>i</i> -alkanes						
ISOBUTAN	Steinbach and Steinbrecher <sup>62</sup>	273-293	0.4-1.1	0.01-0.03	-	12
ISOBUTAN	Robinson et al. <sup>99</sup>	283-394	0.6-20.7	0.01-0.46	0.05-0.94	26
ISOBUTAN	Robinson and Kalra <sup>100</sup>	283-394	0.6-20.7	0.01-0.46	0.05-0.94	26
ISOBUTAN	Kalra et al. <sup>101</sup>	255-394	0.2-20.8	0.01-0.46	0.10-0.97	52
ISOBUTAN	Hudziak et al. <sup>55</sup>	224-350	0.1-5.5	-	0.09-0.74	141
ISOBUTAN	Chen et al. <sup>102</sup>	120-220	0.5-15.0	0.01-0.99	0.97-0.99	58

Continued on next page

Table 2: Available fuel-N<sub>2</sub> vapor-liquid equilibrium literature data obtained from NIST Thermo-DataEngine. Listed with each study are the temperature range ( $T_{\text{range}}$ ), pressure range ( $p_{\text{range}}$ ), liquid ( $x_{\text{N}_2,\text{range}}$ ) and vapor ( $y_{\text{N}_2,\text{range}}$ ) molar composition, and number of data points available ( $n$ ).

Fluid	Study	$T_{\text{range}} / \text{K}$	$p_{\text{range}} / \text{MPa}$	$x_{\text{N}_2,\text{range}}$	$y_{\text{N}_2,\text{range}}$	$n$
IPENTANE	Krishnan et al. <sup>103</sup>	278-377	0.2-20.8	<0.01-0.44	0.16-0.99	47
NEOPENTN	Reisig and Schneider <sup>104</sup>	212-294	3.1-82.6	0.06-0.76	0.84-0.95	111
IOCTANE	Prausnitz and Benson <sup>88</sup>	323-348	2.4-8.5	-	0.98-0.99	8
IOCTANE	Peter and Eicke <sup>77</sup>	376-453	2.0-61.8	0.03-0.75	0.65-0.98	46
IOCTANE	Hesse et al. <sup>105</sup>	298	0.1	<0.01	-	1
IOCTANE	Zhang and Lee <sup>106</sup>	270-282	2.7-9.4	0.05-0.17	-	15
ISOC16	Rowane et al. <sup>98</sup>	298-576	7.9-114.6	0.15-0.87	0.89	34
naphthenes						
CYCLOPEN	Marathe and Sandler <sup>107</sup>	366-410	1.4-31.3	0.02-0.37	0.60-0.90	31
CYCLOHEX	Wilhelm and Battino <sup>108</sup>	283-298	0.1	<0.01	-	3
CYCLOHEX	Vosmansky and Dohnal <sup>109</sup>	288-308	0.1	<0.01	-	3
CYCLOHEX	Shibata and Sandler <sup>110</sup>	366-411	1.8-27.6	0.01-0.29	0.71-0.97	26
CYCLOHEX	Gao et al. <sup>111</sup>	366-411	2.1-12.1	0.02-0.12	-	16
C1CC6	Peter and Eicke <sup>77</sup>	376-453	2.0-88.3	0.02-0.81	0.76-0.98	40
C1CC6	Lebedeva et al. <sup>112</sup>	323-473	2.7-22.5	0.03-0.30	-	22
C1CC6	Brunner et al. <sup>78</sup>	453-497	5.2-37.1	0.06-0.65	0.66-0.91	21
C1CC6	Robinson et al. <sup>113</sup>	311-478	0.4-16.9	0.01-0.27	0.44-0.99	56
C3CC6	Laugier et al. <sup>114</sup>	314-473	1.6-99.7	0.02-0.46	0.84-0.99	60
C3CC6	Richon et al. <sup>115</sup>	314-473	1.6-99.7	0.02-0.46	0.84-0.99	60
JP-10	Liu et al. <sup>116</sup>	293-334	1.7-4.8	0.01-0.03	-	24
TDEC	Gao et al. <sup>111</sup>	344-411	3.7-14.6	0.03-0.11	-	18
CYCLODODEC	Lebedeva et al. <sup>117</sup>	408-473	10.7-17.9	0.08-0.17	-	13
aromatics						
BENZENE	Lewis and Luke <sup>118</sup>	373-473	7.6-9.9	0.04-0.06	0.74-0.97	20
BENZENE	Miller and Dodge <sup>119</sup>	303-423	6.2-30.7	0.03-0.24	0.92-0.98	40
BENZENE	Gamburg <sup>120</sup>	303-348	5.0-49.1	-	0.97-0.99	19
BENZENE	Coan and King <sup>121</sup>	308-323	2.3-6.5	-	0.98-0.99	23
BENZENE	Llave and Chung <sup>81</sup>	303-373	6.7-35.6	0.03-0.20	0.93-0.99	15
BENZENE	de Leeuw et al. <sup>122</sup>	352-445	3.5-167.3	0.04-0.65	0.70-0.95	187
BENZENE	Gao et al. <sup>111</sup>	373-411	3.2-15.8	0.02-0.10	-	15
BENZENE	Jabloniec et al. <sup>75</sup>	303-363	0.2-3.7	<0.01-0.02	-	12
BENZENE	Tsuji et al. <sup>123</sup>	293-313	1.9-3.5	0.01	-	15
BENZENE	Lai et al. <sup>124</sup>	303	1.1-3.3	0.01	-	5
TOLUENE	Prausnitz and Benson <sup>88</sup>	323-348	2.1-6.1	-	0.98-0.99	7
TOLUENE	Laugier et al. <sup>125</sup>	313-473	2.2-100.0	0.02-0.39	0.61-0.99	65
TOLUENE	Llave and Chung <sup>81</sup>	323-348	3.6-35.4	0.02-0.16	-	12
TOLUENE	Richon et al. <sup>115</sup>	313-473	2.2-100.0	0.02-0.39	0.61-0.99	63
TOLUENE	Schlichting et al. <sup>83</sup>	241-282	0.3-10.5	-	0.99	27
TOLUENE	Lin et al. <sup>126</sup>	424-545	5.1-15.2	0.04-0.22	0.43-0.94	40
TOLUENE	Jabloniec et al. <sup>75</sup>	303-363	0.2-2.9	<0.01-0.02	-	12

Continued on next page

Table 2: Available fuel-N<sub>2</sub> vapor-liquid equilibrium literature data obtained from NIST Thermo-DataEngine. Listed with each study are the temperature range ( $T_{\text{range}}$ ), pressure range ( $p_{\text{range}}$ ), liquid ( $x_{\text{N}_2,\text{range}}$ ) and vapor ( $y_{\text{N}_2,\text{range}}$ ) molar composition, and number of data points available ( $n$ ).

Fluid	Study	$T_{\text{range}} / \text{K}$	$p_{\text{range}} / \text{MPa}$	$x_{\text{N}_2,\text{range}}$	$y_{\text{N}_2,\text{range}}$	$n$
PXYLENE	de Leeuw et al. <sup>122</sup>	318-447	5.4-241.2	0.05-0.74	0.80-0.94	265
124MBEN	Bian et al. <sup>127</sup>	298	0.1	<0.01	-	1
135MBEN	Laugier et al. <sup>125</sup>	313-473	1.1-99.8	0.02-0.34	0.78-0.99	57
135MBEN	Richon et al. <sup>115</sup>	313-473	1.1-99.8	0.02-0.34	0.78-0.99	60
C3BEN	Chareton et al. <sup>128</sup>	313-473	2.0-39.7	0.01-0.36	0.92-0.99	48
C3BEN	Renon et al. <sup>129</sup>	313-473	1.0-39.7	0.01-0.36	0.92-0.99	32
MXYLENE	Laugier et al. <sup>125</sup>	313-473	1.1-100.1	0.02-0.35	0.77-0.99	59
MXYLENE	Richon et al. <sup>115</sup>	313-473	1.1-100.1	0.02-0.35	0.77-0.99	58
MXYLENE	Lin et al. <sup>130</sup>	465-585	5.1-15.2	0.05-0.28	0.38-0.94	40
1MNAPHTH	Lin et al. <sup>131</sup>	462-703	2.0-25.4	0.01-0.29	0.47-0.99	27
1MNAPHTH	Gao et al. <sup>111</sup>	344-411	5.0-21.4	0.02-0.08	-	18
NAPHTH	de Leeuw et al. <sup>122</sup>	371-443	10.9-165.1	0.05-0.30	-	43
NAPHTH	Gao et al. <sup>111</sup>	378-411	6.2-18.8	0.03-0.07	-	12
PHENANTH	Gao et al. <sup>111</sup>	383-411	10.4-21.4	0.02-0.05	-	12
PYRENE	Gao et al. <sup>111</sup>	433	7.6-22.9	0.02-0.05	-	6
tetralins						
TETRALIN	Kim et al. <sup>132</sup>	464-663	2.1-25.6	0.02-0.57	0.49-0.99	25

## 2.2 Perturbed Chain Statistical Associating Fluid Theory

PC-SAFT, developed by Gross and Sadowski,<sup>11</sup> is a form of a Helmholtz-energy-explicit EoS derived from the hard-chain potential function. Fig. 3 is a schematic describing how molecules are described by the PC-SAFT EoS, in which hard spheres within a molecule are connected to form hard chain segments, which interact through dispersion interactions. PC-SAFT can also consider association interactions for systems that hydrogen bond. However, no molecules in the scope of this study exhibit association.

$$\tilde{a}^{res} = \bar{m}\tilde{a}^{hs} + \tilde{a}^{chain} + \tilde{a}^{disp} + \tilde{a}^{assoe} \quad (1)$$

For brevity, the equations for each of the contributions are not discussed here and can be found in the study of Gross and Sadowski.<sup>11</sup> The focus of this study is on the parameterization of the model to distill structure-property trends. The three pure-component PC-SAFT parameters are related to molecular structure and are segment length ( $m$ ), the segment diameter ( $\sigma$ ), and the segment energy ( $\epsilon$ ). To obtain an internally consistent set of parameters we utilize the group contribution method of Sauer et al.<sup>133</sup> to estimate  $m$ ,  $\sigma$ , and  $\epsilon$ . Table 3 lists the parameters used for calculations for all chemical species investigated here.

For mixture calculations, a set of  $m$ ,  $\sigma$ , and  $\epsilon$  parameters are needed for each component present in the mixture. PC-SAFT uses the conventional Lorentz-Berthelot mixing rules given by

$$\bar{m} = \sum_i x_i m_i \quad (2)$$

$$\sigma_{ij} = \frac{1}{2} (\sigma_i + \sigma_j) \quad (3)$$

$$\epsilon_{ij} = \sqrt{\epsilon_i \epsilon_j} (1 - k_{ij}) \quad (4)$$

where  $k_{ij}$  in Eq. (4) is the binary interaction parameter. It is interesting to note that  $k_{ij}$  only influences the dispersion contribution of the PC-SAFT EoS and has no impact on the

hard-chain contribution. In this work  $k_{ij}$  values were fitted to experimental data for each binary mixture. Fig. 4 provides sample code for a  $p - xy$  trace at 370 K for the  $n$ -decane- $N_2$  system. The general procedure for tracing an isotherm in the `teqp` python package is to first build models for component 1 and the mixture. Tracing starts from the component 1 pure endpoint, which is obtained using PC-SAFT superancillary equations.<sup>134</sup> `teqp` returns the traced isotherm as a pandas DataFrame that can be plotted using standard plotting packages.

## 3 Results and Discussion

### 3.1 Fitted $k_{ij}$ Values

Fig. 5 shows isothermal  $p - xy$  traces using the PC-SAFT EoS with the parameters and fitted  $k_{ij}$  values listed in Table 3. The  $k_{ij}$  values were obtained from a fit of experimental data to a single isotherm. The isotherm chosen for fitting was that closest to a reduced temperature ( $T_r = T/T_c$ ) of 0.6 for the fuel component to be consistent for all mixtures. However, in some instances sufficient data for fitting was not available at  $T_r = 0.6$ , and in these cases the nearest temperature with at least 5 data points was selected. In select cases a specific isotherm was chosen that provided quality  $p - xy$  traces for the entirety of the data available. VLE data sets listed in Table 2 were either measured at a constant temperature (isotherm) or at a constant composition (isopleth). VLE data sets measured along isopleths rather than isotherms report data at fewer compositions and more unique temperatures. Measurements are typically not performed at the same set of temperatures for each isopleth so isothermal data cannot be obtained immediately. To obtain the  $pxy$  isotherms from the isopleth data shown in Fig. 5 the data were cross-plotted by fitting each isopleth to a polynomial and interpolating at the desired temperature. Table 3 lists the each fuel component’s chemical family, REFPROP name, IUPAC name, CAS number, PC-SAFT parameters, fitted  $k_{ij}$  value, temperature selected for fitting, and either the number of

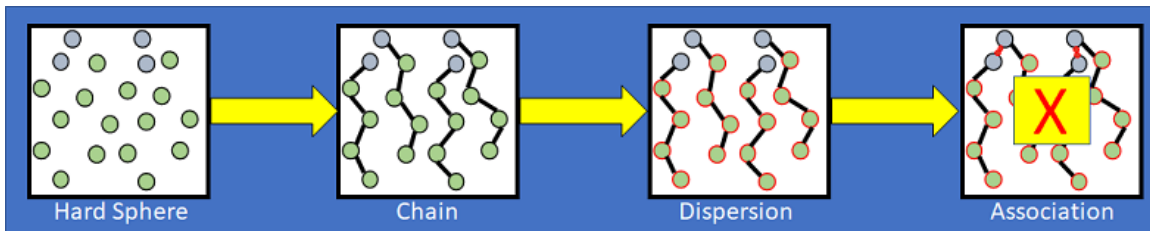


Figure 3: Perturbed-Chain Statistical Associating Fluid Theory (PC-SAFT) where molecules are treated as hard chains, in which hard spheres are bonded together. Neighboring hard chain molecules interact through dispersion. The association interaction is not considered in the scope of this study since none of these molecules in this study exhibit hydrogen bonding.

isothermal data points fit ( $n_{\text{data},T}$ ) or number  
of isopleth data points fit ( $n_{\text{data},x}$ ).

```

import teqp
import PCSAFTsuperanc
import pandas as pd
import numpy as np
import matplotlib.pyplot as plt

coeffs0 = {
    "name": "DECANE",
    "BibTeXKey": 'SauerGC',
    "m": 4.872,
    "epsilon_over_k": 236.722, # [K]
    "sigma_Angstrom": 3.844,
}

# Build pure component model
model0 = teqp.make_model({
    "kind": 'PCSAFT',
    "model": {
        "coeffs": [coeffs0]
    }
})

# Set binary interaction parameter
k_ij = 0.149
kmat = [[0, k_ij], [k_ij, 0]]

# Build mixture model
model = teqp.make_model({
    "kind": 'PCSAFT',
    "model": {
        "coeffs": [coeffs0,
            {
                "name": "NITROGEN",
                "BibTeXKey": 'PCSAFT2001',
                "m": 1.205,
                "epsilon_over_k": 90.960, # [K]
                "sigma_Angstrom": 3.313,
            }
        ],
        "kmat": kmat
    }
})

#Set trace temperature
T = 370

#Superancillaries for pure component endpoint
m = model0.get_m()[0]
Ttilde = T/model0.get_epsilon_over_k_K()[0]
sigma_m = model0.get_sigma_Angstrom()[0]/1e10
Ttilde_crit, Ttilde_min = PCSAFTsuperanc.get_Ttilde_crit_min(m)
[tilderhoL, tilderhoV] = PCSAFTsuperanc.PCSAFTsuperanc_rhoLV(Ttilde, m)
N_A = PCSAFTsuperanc.N_A
rhoL0, rhoV0 = [tilderho/(N_A*sigma_m**3) for tilderho in [tilderhoL, tilderhoV]]

opt = teqp.TVLEOptions(); opt.calc_criticality = True; opt.max_steps=100000;opt.polish=True;
opt.crit_termination=1e-6; opt.p_termination=300e6

#Trace the isotherm and return as data frame
dfT = pd.DataFrame(model.trace_VLE_isotherm_binary(T, np.array([rhoL0,0]), np.array([rhoV0,0]),opt))

dfT['too_critical'] = dfT.apply(lambda row: abs(row['crit. conditions L'])[0] < 5e-6, axis=1)
first_too_critical = np.argmax(dfT['too_critical'])
dfT = dfT.iloc[0:(first_too_critical if first_too_critical else len(dfT))]

dfT['too_highp'] = dfT.apply(lambda row: row['pL / Pa'] > 300e6, axis=1)
first_too_highp = np.argmax(dfT['too_highp'])
dfT = dfT.iloc[0:(first_too_highp if first_too_highp else len(dfT))]

#Plot the data
plt.plot(dfT['xL_0 / mole frac.'], dfT['pL / Pa']/1e6, color='r', lw=1)
plt.plot(dfT['xV_0 / mole frac.'], dfT['pV / Pa']/1e6, dashes=[2,2], color='b', lw=1)
plt.xlabel('$x_{1}, y_{1}$ / mole frac.')
plt.ylabel('p / MPa')
plt.yscale('log')
plt.title('Decane(1) + Nitrogen(2) '+' ('+ str(T)+' K)')

```

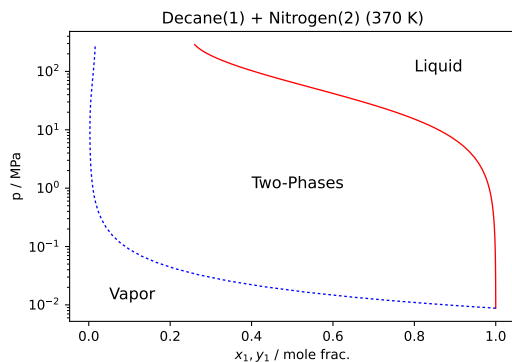


Figure 4: Sample python code used to build a PC-SAFT model for the  $n$ -decane- $N_2$  system, trace a single isotherm, and plot the results.



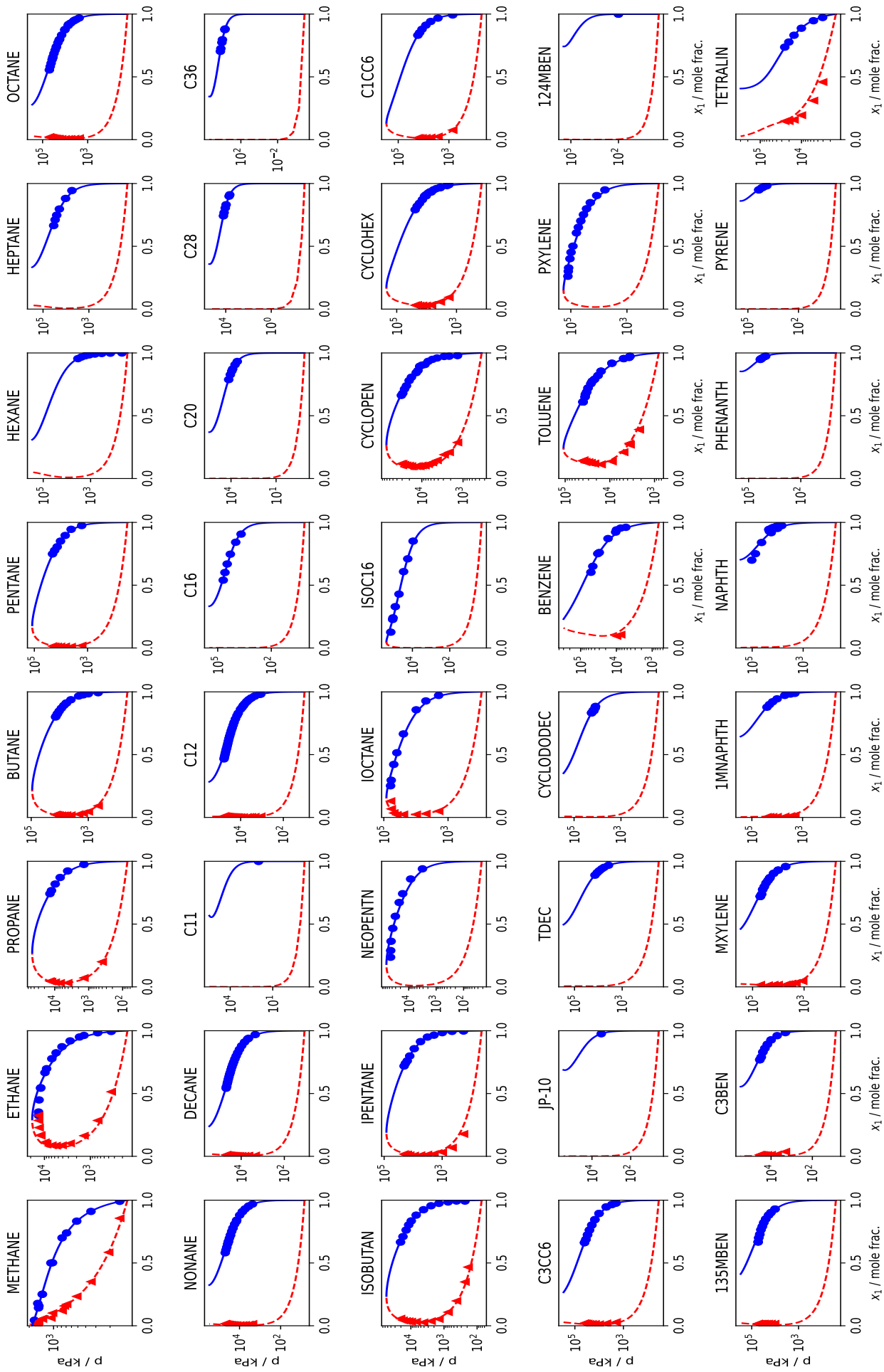


Figure 5: Pressure ( $p$ ) versus mass fraction ( $x_1$ ) traces with fitted  $k_{ij}$  values. Labels above each trace are for the fuel component in the fuel- $N_2$  mixture. Component 1 refers to the fuel component in the mixture. Blue circles are experimental bubble point and red triangles are experimental dew points. Solid lines represent the calculated bubble line and dashed lines represent the calculated dew line.

Table 3: PC-SAFT parameters and relevant thermodynamic data for compounds investigated in this study.

Family	Name	CAS	MW / g·mol <sup>-1</sup>	<i>m</i>	$\sigma / \text{Å}$	$\varepsilon/k / \text{K}$	$k_{ij}$	$T_{\text{fit}} / \text{K}$	$n_{\text{data},T}$	$n_{\text{data},x}$
alkanes	ETHANE	74-84-0	30.07	1.224	3.702	229.900	0.0	194	15	-
alkanes	PROPANE	74-98-6	44.10	1.680	3.755	232.373	0.063	223	6	-
alkanes	BUTANE	106-97-8	58.12	2.136	3.785	233.790	0.095	250	14	-
alkanes	PENTANE	109-66-0	72.15	2.592	3.804	234.708	0.102	277	7	-
alkanes	HEXANE	110-54-3	86.18	3.048	3.817	235.352	0.141	304	8	-
alkanes	HEPTANE	142-82-5	100.20	3.504	3.826	235.828	0.151	324	6	-
alkanes	OCTANE	111-65-9	114.23	3.960	3.834	236.195	0.147	344	23	-
alkanes	NONANE	111-84-2	128.26	4.416	3.840	236.485	0.15	344	22	-
alkanes	DECANE	124-18-5	142.28	4.872	3.844	236.722	0.149	377	22	-
alkanes	C11	1120-21-4	156.31	5.328	3.848	236.917	0.158	298	1	-
alkanes	C12	112-40-3	170.33	5.785	3.852	237.082	0.177	411	35	-
alkanes	C16	544-76-3	226.45	7.609	3.861	237.545	0.199	423	6	-
alkanes	C20	112-95-8	282.55	9.433	3.867	237.828	0.218	423	6	-
alkanes	C28	630-02-4	394.76	13.082	3.873	238.158	0.226	423	6	-
alkanes	C36	630-06-8	506.97	16.730	3.877	238.344	0.234	423	6	-
ialkanes	ISOBUTAN	75-28-5	58.12	1.979	3.811	238.410	0.066	255	12	-
ialkanes	IPENTANE	78-78-4	72.15	2.435	3.826	238.523	0.086	278	11	-
ialkanes	NEOPENTN	463-82-1	72.15	1.778	4.160	275.955	0.071	250	-	9
ialkanes	IOCTANE	540-84-1	114.23	2.989	4.076	264.319	0.102	376	8	-
ialkanes	ISOC16	4390-04-9	226.44	5.009	4.262	284.791	0.121	415	-	8
naphthenes	CYCLOPEN	287-92-3	70.13	2.337	3.727	267.160	0.072	366	17	-
naphthenes	CYCLOHEX	110-82-7	84.16	2.370	3.913	289.030	0.131	366	16	-
naphthenes	C1CC6	108-87-2	98.19	2.616	4.022	286.401	0.137	353	7	-
naphthenes	C3CC6	1678-92-8	126.24	3.528	3.989	274.147	0.161	393	20	-
naphthenes	JP-10	2825-82-3	136.23	2.775	4.344	316.544	0.286	334	1	-
naphthenes	TDEC	493-02-7	138.25	3.217	4.156	307.250	0.24	411	6	-
naphthenes	CYCLODODEC	294-62-2	168.32	4.740	3.913	289.030	0.182	473	7	-
aromatics	BENZENE	71-43-2	78.11	2.540	3.727	274.410	0.167	423	9	-
aromatics	TOLUENE	108-88-3	92.14	2.882	3.735	278.440	0.151	473	30	-

Continued on next page

Table 3: PC-SAFT parameters and relevant thermodynamic data for compounds investigated in this study.

Family	Name	CAS	MW / g·mol <sup>-1</sup>	<i>m</i>	$\sigma / \text{Å}$	$\varepsilon/k / \text{K}$	$k_{ij}$	$T_{\text{fit}}/K$	$n_{\text{data},T}$	$n_{\text{data},x}$
aromatics	PXYLENE	106-42-3	106.17	3.225	3.741	281.615	0.082	400	-	14
aromatics	124MBEN	95-63-6	120.19	3.567	3.746	284.180	0.146	298	2	-
aromatics	135MBEN	108-67-8	120.19	3.567	3.746	284.180	0.133	393	20	-
aromatics	C3BEN	103-65-1	120.19	5.019	3.756	259.435	0.21	403	14	-
aromatics	MXYLENE	108-38-3	106.17	3.225	3.741	281.615	0.155	392	24	-
aromatics	1MNAPHTH	90-12-0	142.20	4.037	3.752	296.540	0.25	462	7	-
aromatics	NAPHTH	91-20-3	128.17	3.694	3.748	295.446	0.267	440	-	17
aromatics	PHENANTH	85-01-8	178.23	4.848	3.758	306.467	0.329	411	6	-
aromatics	PYRENE	129-00-0	202.25	5.156	3.771	319.629	0.349	433	6	-
tetralins	TETRALIN	119-64-2	132.20	3.581	3.832	302.564	0.295	623	6	-
gas	NITROGEN	7727-37-9	28.01	1.205	3.313	90.960	-	-	-	-

Fig. 6 (a) and (b) show the average nitrogen mole fraction residual given by,

$$x_{\text{res,avg}} = \frac{1}{N} \sum_{n=1}^N |x_{\text{N}_2,\text{exp}} - x_{\text{N}_2,\text{calc}}| \quad (5)$$

for liquid ( $x_{\text{res,avg}}$ ) and vapor ( $y_{\text{res,avg}}$ ) phases, respectively when comparing the PC-SAFT EoS using the fitted  $k_{ij}$  values. Numbers at the top of each bar in Fig. 6 (a) represent the number of data points missed by the  $p - xy$  trace, which occurs when the EoS predicts a single phase at a given pressure and temperature. For all systems in the liquid phase the  $x_{\text{res,avg}}$  values are less than 0.07 mole fraction. However, it should be noticed that a majority of the systems have  $x_{\text{res,avg}}$  values lower than 0.04 mole fraction with the exclusion of ethane, neopentane, benzene, and  $p$ -xylene. A similar trend is seen for these systems in the vapor phase with a majority of  $y_{\text{res,avg}}$  values being less than 0.08 mole fraction with a majority of the  $y_{\text{res,avg}}$  values lower than 0.04 mole fraction. For vapor phase compositions the major outliers are 2,2,4,4,6,8,8-heptamethylnonane (ISOC16) and 1-methylnaphthalene (1MNAPHTH).

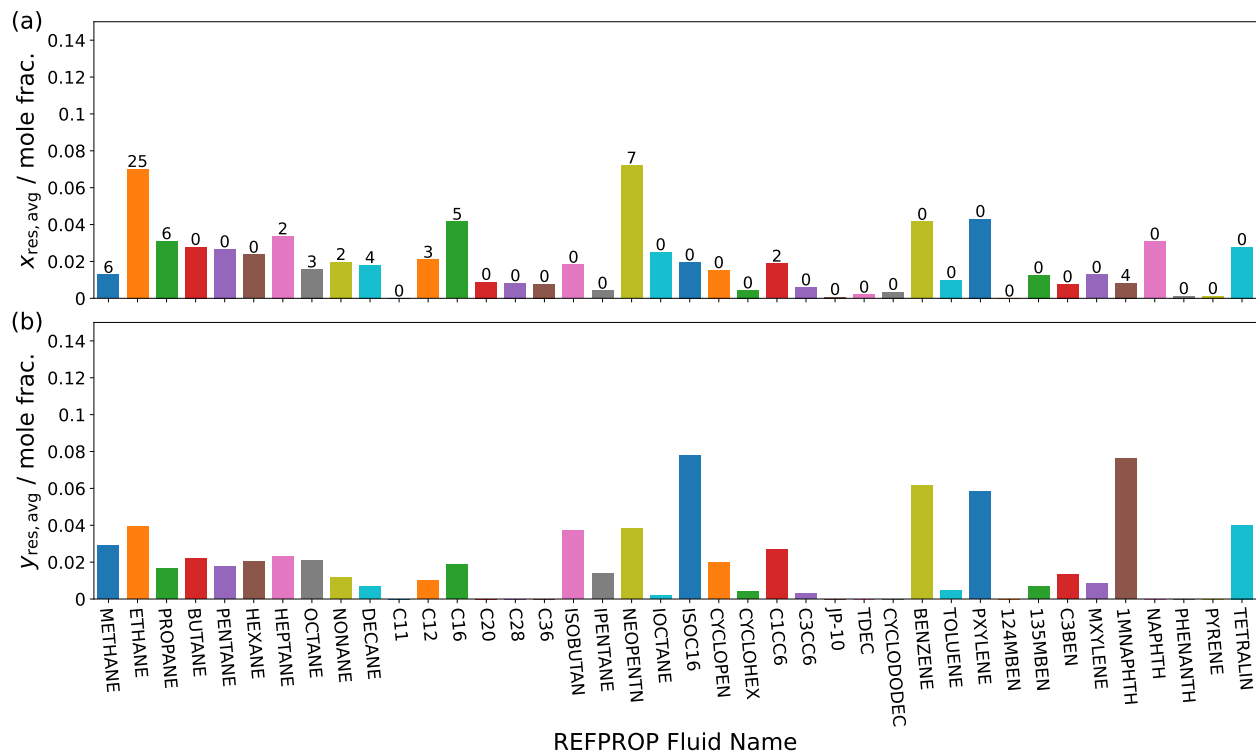


Figure 6: Average (a) liquid and (b) vapor phase mole fraction residual for PC-SAFT calculations using fitted  $k_{ij}$  values. Numbers at the top of each bar in (a) are the number of points missed when tracing all isotherms. The mole fraction residual used in this figure is defined by equation 5.

An inherent weakness of group contribution methods is that they may produce sub-optimal parameters for structurally complex fluids. In this study neopentane was chosen as a case study to highlight these shortcomings of group contribution methods. Fig. 7 compares the performance of the PC-SAFT EoS when using two different sets of PC-SAFT  $m$ ,  $\sigma$ , and  $\epsilon/k$  parameters. Fig. 7 (a) uses group contribution parameters estimated from the GC method of Sauer et al.<sup>133</sup> and Fig. 7 (b) uses PC-SAFT parameters obtained by fitting the EoS of Lemmon and Span<sup>135</sup> included in REFPROP version 10.0.<sup>9</sup> Fig. 7 (a) shows that fitting a single  $k_{ij}$  value the PC-SAFT EoS with the group contribution parameters does not provide the best representation of the vapor-liquid equilibrium across all temperatures. However, as shown in Fig. 7 (b) a slightly better result can be obtained when parameters are fit to more faithfully represent the properties of pure fluids. It is important to note that due to limitations of the EoS in the case of neopentane it is still not possible to yield a reliable characterization of mixture properties. Similar challenges were encountered for N<sub>2</sub> mixtures with both *p*-xylene and benzene. The  $p - xy$  traces for these systems can be found in the supporting information.

The ethane-N<sub>2</sub> system exhibits type III phase behavior, which includes vapor-liquid, liquid-liquid, and vapor-liquid-liquid equilibrium.<sup>136</sup> Greater deviations seen in Fig. 6 (a) and (b) are not surprising given the challenges in modeling such a system. Fig. 8 shows modeling results for the ethane-nitrogen systems using the PC-SAFT EoS with fitted  $k_{ij}$  parameters. Fig. 8 not only shows vapor-liquid  $p - xy$  loops but shows discontinuous  $p - xy$  traces approaching a local maximum at lower temperatures, which are actually predictive liquid-liquid equilibrium results. It is important to note that none of the experimental data points plotted in Fig. 8 are for liquid-liquid equilibrium. This demonstrates that despite the weaknesses of PC-SAFT in providing reference quality predictions of thermodynamic properties the EoS is capable of qualitatively predicting the phase behavior of complex systems.

$p - xy$  traces for all available data sets are included in the supporting information. In the next section a generalized correlation for the fuel-N<sub>2</sub>  $k_{ij}$  values is presented.

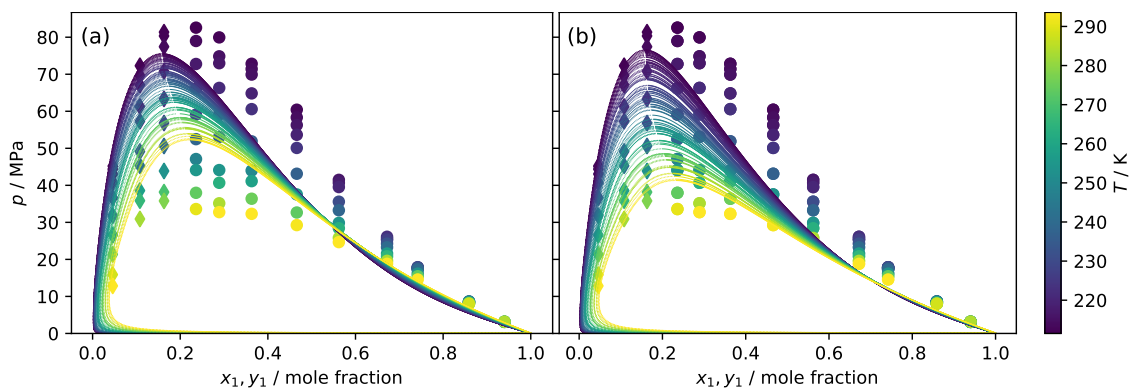


Figure 7:  $p - xy$  traces for the neopentane + nitrogen system with fitted  $k_{ij}$  values. (a) Neopentane parameters were estimated from the GC method of Sauer et al.<sup>133</sup> and (b) parameters were obtained by fitting the PC-SAFT EoS to calculated points from the reference equation of Lemmon and Span.<sup>135</sup> Note that the intent of this figure is to demonstrate the overall agreement of the model with the experimental data by showing the proximity of the data points to the traced isotherm.

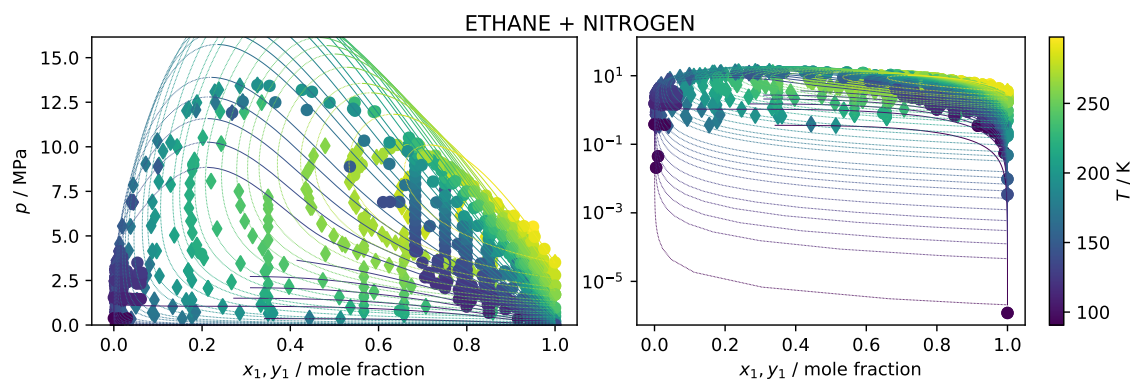


Figure 8:  $p - xy$  traces for the ethane + nitrogen system with fitted  $k_{ij}$  value. Note that the intent of this figure is to demonstrate the overall agreement of the model with the experimental data by showing the proximity of the data points to the traced isotherm. All isothermal traces displayed in the figure are included in the SI in the form of .csv files contained in the zipped folder named csvtraces.

### 3.2 Correlated $k_{ij}$ Values

Fig. 9 shows the relationship between the fitted  $k_{ij}$  values as a function of molar mass where different symbols represent the different chemical families investigated. There is a distinct power law trend for both the  $n$ -alkanes and polynuclear aromatic (PNA) components (benzene, naphthalene, phenanthrene, and pyrene). The trends for  $i$ -alkanes, naphthenes, and branched aromatics exhibit less distinct trends. However, it can be observed in Fig. 9 that  $i$ -alkanes and branched aromatics exhibit lower  $k_{ij}$  values than their non-branched counterparts. For the systems of interest in this study, at a fixed molar mass, larger  $k_{ij}$  values indicate less mutual solubility between the fuel component and nitrogen and mixture critical points occurring at higher temperatures.

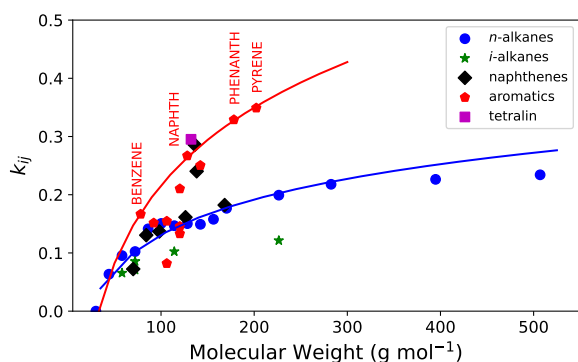


Figure 9: Fitted  $k_{ij}$  values for different chemical families investigated. Blue line is an exponential fit of the  $n$ -alkane  $k_{ij}$  values. The red line is an exponential fit of the polynuclear aromatics  $k_{ij}$  values that are both explicitly labeled and displayed in red on the plot.

A correlation to approximate  $k_{ij}$  values for the different chemical families found in fuels with nitrogen can be developed. Rokni et al.<sup>137</sup> demonstrated that PC-SAFT parameters at a fixed molar mass vary with the degree of unsaturation (DoU) given by,

$$\text{DoU} = \frac{1}{2}(2 \cdot N_C + 2 - N_H) \quad (6)$$

where  $N_C$  and  $N_H$  are the number of carbon and hydrogen atoms in the molecule. In the absence of branching and fixed  $N_C$ , the DoU

varies from 0 for alkanes to a maximum value given by,

$$\text{DoU}_{\text{PNA}} = 0.599 \cdot MW - 0.682 \quad (7)$$

for PNAs. Values of saturated ring structures, tetralins/indanes, and aromatics with branching exhibit DoU values between those of alkanes and PNAs. The parameter  $Z$  given by

$$Z = \frac{\text{DoU}_{\text{component}}}{\text{DoU}_{\text{PNA}}} \quad (8)$$

provides a relative value for the DoU, which is the ratio between the DoU for a given component,  $\text{DoU}_{\text{component}}$ , and the  $\text{DoU}_{\text{PNA}}$  at the same molar mass. Using the power law functions for  $n$ -alkanes and PNAs and the parameter  $Z$  a  $k_{ij}$  value can be estimated by,

$$k_{ij,\text{NBC}} = (1 - Z)[0.08759 \ln(MW) - 0.27236] + Z[0.19296 \ln(MW) - 0.67264] \quad (9)$$

A weakness of this approach is that it does not include a term that explicitly considers the impact of branching on  $k_{ij}$ . The quantities  $MW$  and DoU are the same for structural  $n$ -paraffins and  $i$ -paraffins. As shown in Fig. 9 the  $k_{ij}$  values for these two chemical families vary significantly at a fixed  $MW$ . Fig. 10 shows the deviation between  $k_{ij}$  values fit to experimental data to those estimated using Eq. (9) plotted against the square of the fraction of  $MW$  attributed to branching. Fitting a linear relationship through the deviation while fixing the y-intercept to zero yields,

$$k_{ij,\text{BC}} = k_{ij,\text{NBC}} - 0.30911x^2 \quad (10)$$

with

$$x = \frac{15.04n_{\text{CH}_3} + 14.03n_{\text{CH}_2}}{MW} \quad (11)$$

where  $n_{\text{CH}_3}$  and  $n_{\text{CH}_2}$  are the number of  $\text{CH}_3$  and groups on a branching segment. The form of the branching contribution is zero for molecules without branching. Fig. 11 is a parity plot comparing fitted  $k_{ij}$  values to those calculated with Eq. (8) and Eq. (9). Fig. 11 shows that incorporating the branching correc-

tion improves estimated  $k_{ij}$  values for components with branching segments. Calculations with Eq. (9) result in a sum of residuals for branching components ( $\sum |k_{ij,\text{fit}} - k_{ij,\text{NBC}}|$ ) of 0.57. Including the branching correction the residual ( $\sum |k_{ij,\text{fit}} - k_{ij,\text{NBC}}|$ ) is reduced to 0.30.

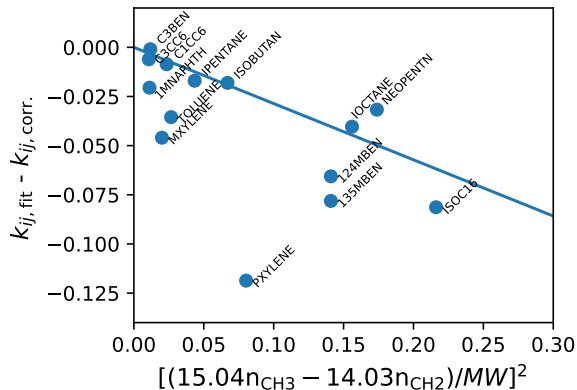


Figure 10: The difference between  $k_{ij}$  values fit to experimental data ( $k_{ij,\text{fit}}$ ) and those calculated using Eq. (9),  $k_{ij,\text{NBC}}$  versus the molar mass fraction attributed to branching. The mole fraction residual used in this figure is defined by equation 5.

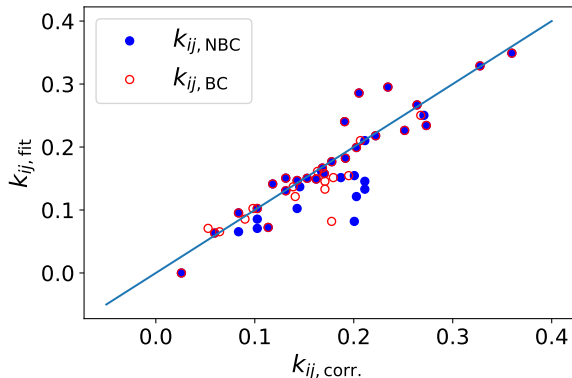


Figure 11: Parity plot of fitted binary interaction parameters to  $k_{ij,\text{fit}}$  those calculated using the correlation without the branching correction,  $k_{ij,\text{NBC}}$ , and with the branching correction,  $k_{ij,\text{BC}}$ .

Fig. 12 (a) and (b) summarize the performance of the PC-SAFT EoS when using the  $k_{ij}$  values estimated from Eq. (10) for liquid and vapor phase compositions, respectively. For liquid phase composition predictions the majority of the  $x_{\text{res,avg}}$  are less than 0.04 mole fraction, which is comparable to values shown in

Fig. 12 (a). However, greater  $x_{\text{res,avg}}$  values for the ethane, neopentane, benzene, and *p*-xylene are obtained when using  $k_{ij}$  from the correlation. Very comparable results are seen in Fig. 12 (b) when calculating vapor phase compositions when using either the correlation or fitted  $k_{ij}$  values. It is interesting to note that although the correlation provides a greater  $x_{\text{res,avg}}$  for ethane no data points were missed across all temperatures.

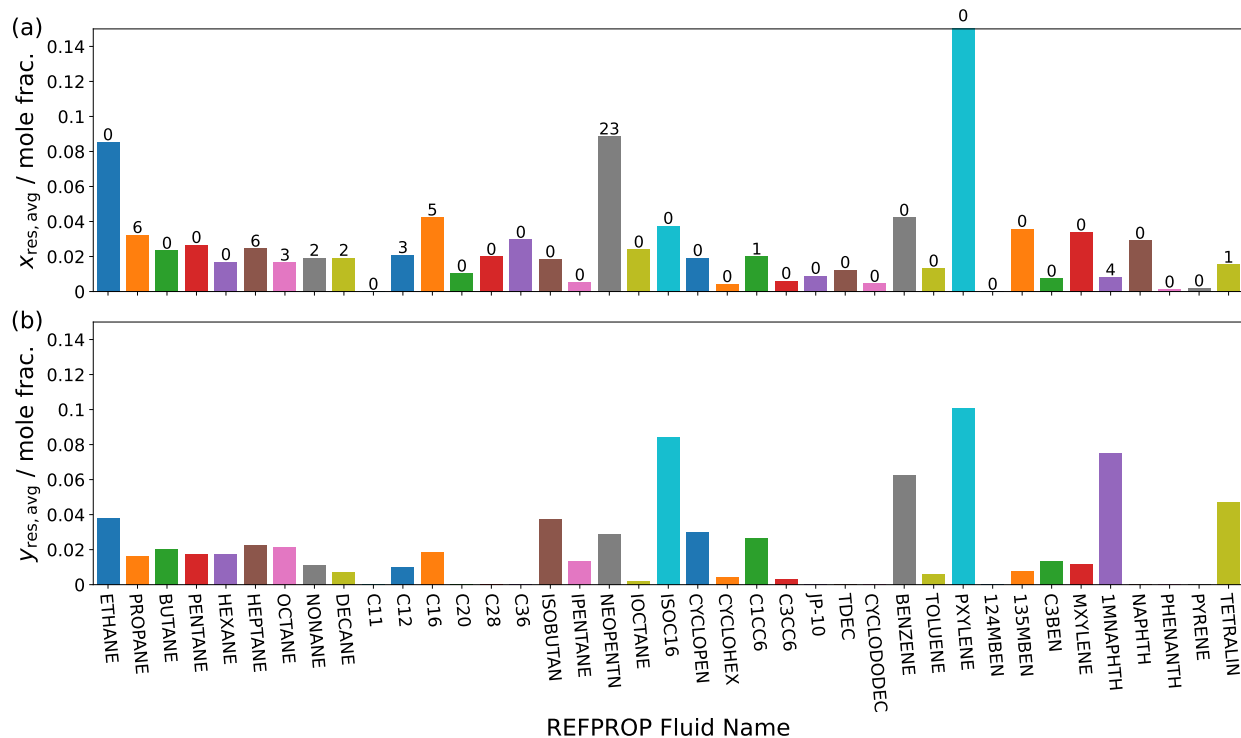


Figure 12: Average (a) liquid and (b) vapor phase mole fraction residual for PC-SAFT calculations using  $k_{ij}$  values calculated with Eq. (10). Numbers at the top of each bar in (a) are the number of points missed when tracing all isotherms.

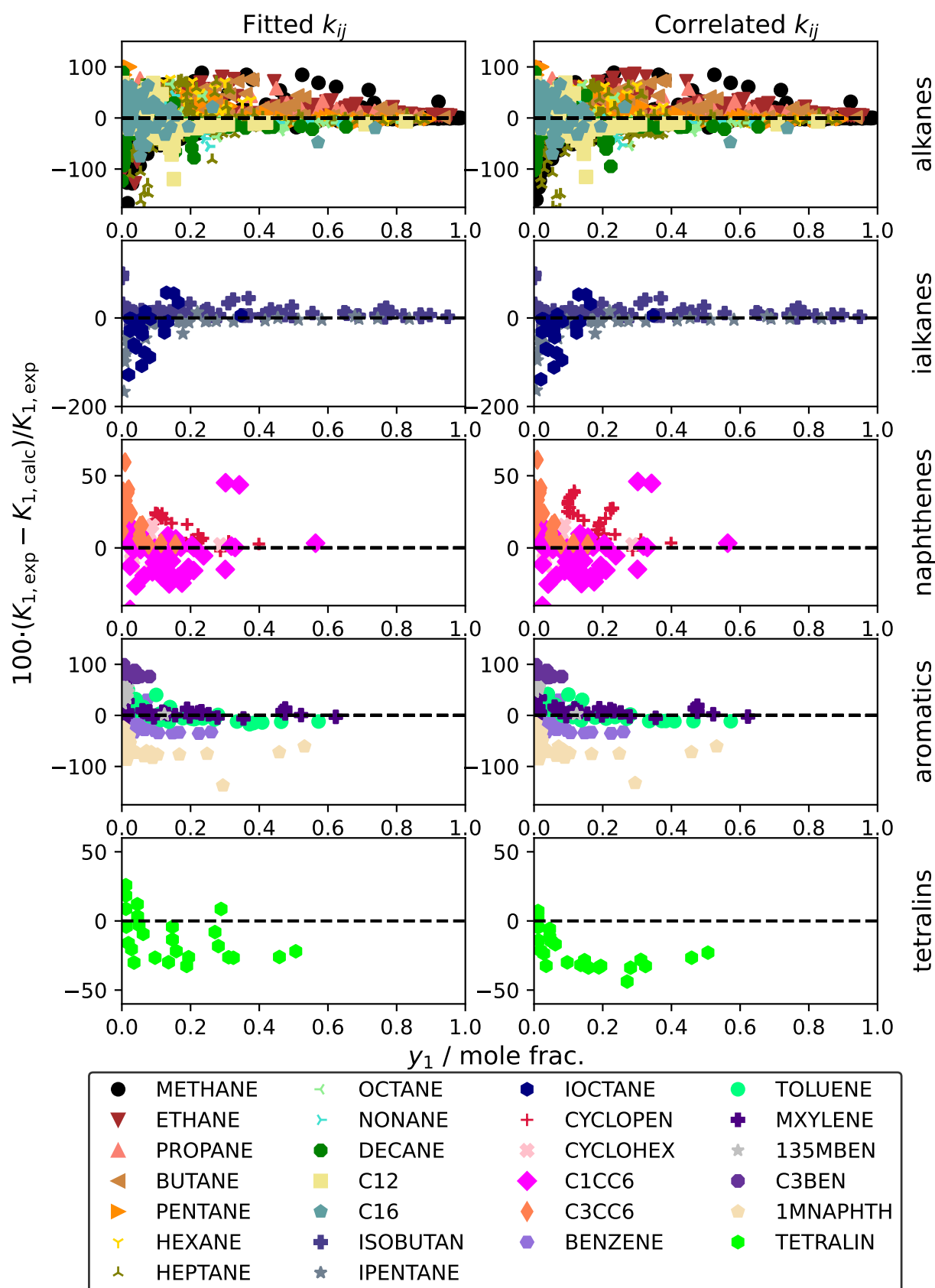


Figure 13: Comparison of experimental relative volatility to that calculated using the PC-SAFT EOS with fitted  $k_{ij}$  values and those calculated using Eq. (10).

Fig. 13 compares the experimental relative volatility of the fuel component,  $K_{1,exp} = y_{1,exp}/x_{1,exp}$ , to that calculated using the PC-SAFT EoS with both fitted and correlated  $k_{ij}$  values,  $K_{1,calc} = y_{1,calc}/x_{1,calc}$ , as a function of the composition of the fuel component in the vapor phase,  $y_1$ . To reduce clutter on the plots the comparisons were organized into the different chemical families. For nearly all chemical families deviations exceeding 100% are observed. The challenges in the modeling and potentially those associated with minimizing the uncertainty in the measurement relative volatility for fuel-N<sub>2</sub> mixtures can be discerned from Fig. 14. The 167% deviation seen for IPENTANE in Fig. 13 occurred as the  $K_1$  approached a minimum of 0.007, which corresponds to a mole fraction of 0.006 for IPENTANE in the vapor phase. These IPENTANE + N<sub>2</sub> data were reported by Krishnan et al.<sup>103</sup> who report what is assumed to be a standard uncertainty of 0.005 mole fraction. This demonstrates that while deviations approaching 200% may seem significant to the unformed reader they are indeed reasonable relative to the uncertainty in the experimental data. Like the study of Krishnan et al.,<sup>103</sup> a majority of the techniques used to obtain coexisting vapor and liquid phases were sampling techniques using gas chromatography with comparable composition uncertainties. Fig. 13 shows a clear trend that the greatest deviations occur as  $y_1$  approaches a value of zero and the detection limit of the fuel component in the vapor phase diminishes.

Fig. 13 also generally reveals that determining  $k_{ij}$  from the correlation does not dramatically increase the model deviations. Increased deviations are seen for a few select systems including that of CYCLOPEN + N<sub>2</sub> and TETRALIN + N<sub>2</sub>. It is challenging to discern if these deviations can be completely attributed to the correlation itself. It is important to reference Fig. 1, which shows that the only available data for CYCLOPEN + N<sub>2</sub> and TETRALIN + N<sub>2</sub> are reported by Marathe and Sandler<sup>107</sup> and Kim et al.,<sup>132</sup> respectively. This is also the case for the NEOPENTN + N<sub>2</sub> and PXYLENE + N<sub>2</sub> systems for which the only data available are reported by Reisig and Schneider<sup>104</sup> and

de Leeuw et al.,<sup>122</sup> respectively. Fig. 6 and Fig. 12 show that the NEOPENTN + N<sub>2</sub> and PXYLENE + N<sub>2</sub> system are outliers exhibiting significantly higher deviations relative to the other systems investigated in this study. Forming a consensus that these deviations can solely be attributed to weaknesses in the PC-SAFT EoS ability to resolve structure property trends would require data sets from multiple sources.

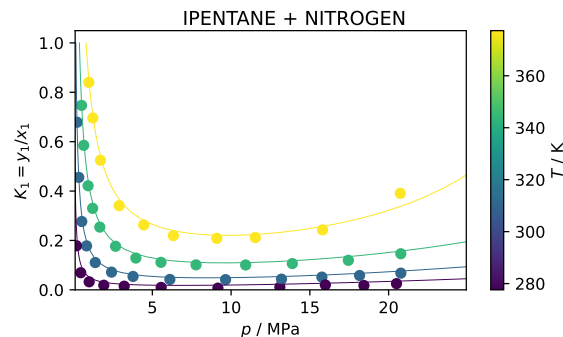


Figure 14: Relationship between the relative volatility of IPENTANE in the IPENTANE + N<sub>2</sub> binary mixture and pressure along several isotherms.

## 4 Conclusions

In this study the fuel-N<sub>2</sub> data included in TDE was evaluated and used to develop a predictive model for the VLE of fuel-N<sub>2</sub> mixtures. The PC-SAFT EoS coupled with a group contribution method provides a reliable method to predict the thermodynamic properties of pure fluids. However, for the highly asymmetric mixtures examined in this study it is imperative that a binary interaction parameter be used to provide reasonable phase behavior predictions. Binary interaction parameters were fitted for each fuel-N<sub>2</sub> system studied and a correlation was developed to provide a predictive method for the vapor-liquid equilibria of N<sub>2</sub> mixtures with *n*-alkanes, *i*-alkanes, naphthenes, aromatics, and tetralins. The performance of the predictive model was comparable to that where fitted  $k_{ij}$  values were used. It was found that the performance of the PC-SAFT EoS was not significantly different when  $k_{ij}$  values calculated from the correlation were used. This study also

highlights the paucity of data available for fuel-N<sub>2</sub> mixtures, which presents challenges when both developing and assessing models. In future studies this method will be expanded to provide predictions for the phase behavior of complex multicomponent fuels with N<sub>2</sub> and surrogate blends more representative of fuels used in modern engines.

## 5 Associated Content

### Supporting Information

Supporting information includes  $p - xy$  traces for all available data for each system studied in graphical form in the file named "SI\_paper". Tabulated modeling data for each trace plotted in "SI\_paper.pdf" is included in the zipped folder "csvtraces.zip".

## 6 Author Information

### Corresponding Author

**Aaron J. Rowane** – Applied Chemicals and Materials Division, National Institute of Standards and Technology, Boulder, CO 80305; orcid.org/0000-0001-7605-0774  
Email: aaron.rowane@nist.gov

### Authors

**Davide Menegazzo** – Department of Industrial Engineering–Applied Physics Section, University of Padova, 35131 Padova, Italy and Construction Technologies Institute, National Research Council (ITC-CNR), 35127 Padova, Italy; orcid.org/0000-0001-9555-4599

**Ian H. Bell** – Applied Chemicals and Materials Division, National Institute of Standards and Technology, Boulder, CO 80305; orcid.org/0000-0003-1091-9080

### Notes

The authors declare no competing financial interest.

### Author Contributions

A.J.R.: Conceptualization, Data curation, Formal analysis, Investigation, Methodology, Visualization, Writing – original draft. D.M.: Formal analysis, Investigation, Writing – review &

editing. I.H.B.: Software, Resources, Supervision, Investigation, Formal analysis, Writing – review & editing.

## 7 Acknowledgments

This work was supported by the National Institute of Standards and Technology.

## Literature Cited

- (1) Bureau of Transportation Statistics Airline Fuel Cost and Consumption (W.S. Carriers - Scheduled) January 2000 - June 2023. <https://transtats.bts.gov/fuel.asp>, 2023; Accessed: 09/01/2023.
- (2) Department of Energy, SAF Grand Challenge Roadmap Flight Plan for Sustainable Aviation Fuel. <https://www.energy.gov/sites/default/files/2022-09/beto-saf-gc-roadmap-report-sept-2022.pdf>, 2022.
- (3) Fahim Shahriar, M.; Khanal, A. The Current Techno-Economic, Environmental, Policy Status and Perspectives of Sustainable Aviation Fuel (SAF). *Fuel* **2022**, *325*, 124905, DOI: 10.1595/205651320X15874763002058.
- (4) Ng, K. S.; Farooq, D.; Yang, A. Global Biorenewable Development Strategies for Sustainable Aviation Fuel Production. *Renew. Sust. Energ. Rev.* **2021**, *150*, 111502, DOI: 10.1016/j.rser.2021.111502.
- (5) Anuar, A.; Undavalli, V.; Khandelwal, B.; Blakey, S. Effect of Fuels, Aromatics and Preparation Methods on Seal Swell. *Aeronaut. J.* **2021**, *125*, 1542–1565, DOI: 10.1017/aer.2021.25.
- (6) Colket, M. et al. Overview of the National Jet Fuels Combustion Program. *AIAA J* **2017**, *55*, 1087–1104, DOI: 10.2514/1.J055361.

- (7) Epstein, A. H. Aircraft Engines' Needs from Combustion Science and Engineering. *Combust. Flame* **2012**, *159*, 1791–1792, DOI: 10.1016/j.combustflame.2012.02.022.
- (8) Huang, D.; Xu, J.; Meng, H. Large Eddy Simulations of Turbulent Combustion of Kerosene-Air in a Dual Swirl Gas Turbine Model Combustor at High Pressures. *Fuel* **2020**, *282*, 118820, DOI: 10.1016/j.fuel.2020.1188202.
- (9) Lemmon, E. W.; Bell, I. H.; Huber, M. L.; McLinden, M. O. NIST Standard Reference Database 23: Reference Fluid Thermodynamic and Transport Properties-REFPROP, Version 10.0, National Institute of Standards and Technology. 2018; <https://www.nist.gov/srd/refprop>.
- (10) Span, R. *Multiparameter Equations of State - An Accurate Source of Thermodynamic Property Data*; Springer, 2000; DOI: 10.1007/978-3-662-04092-8.
- (11) Gross, J.; Sadowski, G. Perturbed-Chain SAFT: An Equation of State Based on a Perturbation Theory for Chain Molecules. *Ind. Eng. Chem. Res.* **2001**, *40*, 1244–1260, DOI: 10.1021/ie0003887.
- (12) Bell, I. H.; Lemmon, E. W. Automatic Fitting of Binary Interaction Parameters for Multi-fluid Helmholtz-Energy-Explicit Mixture Models. *J. Chem. Eng. Data* **2016**, *61*, 3752–3760, DOI: 10.1021/acs.jced.6b00257.
- (13) Deiters, U. K.; Bell, I. H. Unphysical Critical Curves of Binary Mixtures Predicted with GERG Models. *Int. J. Thermophys.* **2020**, *41*, DOI: 10.1007/s10765-020-02743-3.
- (14) McTaggart, H. A.; Edwards, E. Composition of the Vapor and Liquid Phases of the System Methane + Nitrogen. *Trans. R. Soc. Can.* **1919**, *13*, 57–66.
- (15) Torocheshnikov, N.; Levius, M. Liquid Vapor Equilibrium in the System Nitrogen - Methane. *Zh. Khim. Prom-sti* **1941**, *18*, 19–22.
- (16) Bloomer, O. T.; Parent, J. D. Liquid-Vapor Phase Behavior of the Methane-Nitrogen System. *Chem. Eng. Prog. Symp. Ser.* **1953**, *49*, 11–24.
- (17) Cines, M. R.; Roach, J. T.; Hogan, R. J.; Roland, C. H. Nitrogen-Methane Vapor-Liquid Equilibrium. *Chem. Eng. Prog. Symp. Ser.* **1953**, *49*, 1.
- (18) Fastovskii, V. G.; Petrovskii, Y. V. VLE in  $N_2$  + Methane. *Zh. Fiz. Khim.* **1957**, *31*, 2317.
- (19) Brandt, L. W.; Stroud, L. Phase Equilibria in Natural Gas Systems Apparatus with Windowed Cell for 800 P.S.I.G and Temperatures to  $-320^\circ\text{F}$ . *Ind. Eng. Chem.* **1958**, *50*, 849–852, DOI: 10.1021/ie50581a046.
- (20) Cheung, H.; Wang, D. I. J. Solubility of Volatile Gases in Hydrocarbon Solvents at Cryogenic Temperatures. *Ind. Eng. Chem. Fundam.* **1964**, *3*, 355, DOI: 10.1021/i160012a014.
- (21) Sprow, F. B.; Prausnitz, J. M. Vapor-Liquid Equilibria for Five Cryogenic Mixtures. *AIChE J.* **1966**, *12*, 780–784, DOI: 10.1002/aic.690120427.
- (22) Chang, S.-D.; Lu, B. C.-Y. Vapor-Liquid Equilibria in the Nitrogen-Methane-Ethane System. *Chem. Eng. Prog., Symp. Ser.* **63**(81), 1967; pp 18–27.
- (23) Fuks, S.; Bellemans, A. Excess Free Energies and Volumes of Two Simple Binary Liquid Mixtures: Methane + Krypton and Nitrogen + Methane. *Bull. Soc. Chim. Belg.* **1967**, *76*, 290, DOI: 10.1002/bscb.19670760503.
- (24) Skripka, V. G.; Nikitina, I. E.; Zhdanovich, L. A.; Sirotin, A. G.; Ben'yaminovich, O. A. Liquid-Vapor

- Phase Equilibrium at Low Temperatures in Binary Systems Formed by Components of Natural Gas. *Gaz. Prom.* **1970**, *15*, 35–36.
- (25) Miller, R. C.; Kidnay, A. J.; Hiza, M. J. Liquid-Vapor Equilibria at 112.00 K for Systems Containing Nitrogen, Argon, and Methane. *AIChE J.* **1973**, *19*, 145–151, DOI: 10.1002/aic.690190121.
- (26) Stryjek, R.; Chappellear, P. S.; Kobayashi, R. Low-Temperature Vapor-Liquid Equilibria of Nitrogen + Methane System. *J. Chem. Eng. Data* **1974**, *19*, 334–339, DOI: 10.1021/je60063a023.
- (27) Kidnay, A. J.; Miller, R. C.; Parrish, W. R.; Hiza, M. J. Liquid-Vapour Phase Equilibria in the N<sub>2</sub> - CH<sub>4</sub> System from 130 to 180 K. *Cryogenics* **1975**, *15*, 531–540, DOI: 10.1016/0011-2275(75)90149-6.
- (28) Wilson, G. M. Vapor-Liquid Equilibria of Nitrogen, Methane, Ethane, and Propane Binary Mixtures at LNG Temperatures from Total Pressure Measurements. *Adv. Cryog. Eng.* **1975**, *20*, 164–171.
- (29) McClure, D. W.; Lewis, K. L.; Miller, R. C.; Staveley, L. A. K. Excess Enthalpies and Gibbs Free Energies for Nitrogen + Methane at Temperatures Below the Critical Point of Nitrogen. *J. Chem. Thermodyn.* **1976**, *8*, 785–792, DOI: 10.1016/0021-9614(76)90057-4.
- (30) Hiza, M. J.; Haynes, W. M.; Parrish, W. R. Orthobaric Liquid Densities and Excess Volumes for Binary Mixtures of Low Molar-Mass Alkanes and Nitrogen between 105 and 140 K. *J. Chem. Thermodyn.* **1977**, *9*, 873–896, DOI: 10.1016/0021-9614(77)90173-2.
- (31) Kremer, H. Experimental Investigation and Calculation of High-Pressure Liquid-Vapor and Liquid-Liquid-Vapor Equilibria for Low-Boiling Mixtures. Ph.D. thesis, University of Berlin, 1982.
- (32) Kremer, H.; Knapp, H. Vapor-Liquid Equilibria in Ternary Mixtures of H<sub>2</sub>, N<sub>2</sub>, CO and CH<sub>4</sub>. *Fluid Phase Equilib.* **1983**, *11*, 289–310, DOI: 10.1016/0378-3812(83)85030-4.
- (33) Llave, F. M.; Luks, K. D.; Kohn, J. P. Three-Phase Liquid-Liquid-Vapor Equilibria in the Nitrogen-Methane-Ethane and Nitrogen-Methane-Propane Systems. *J. Chem. Eng. Data* **1987**, *32*, 14–17, DOI: 10.1021/je00047a004.
- (34) Liu, K.; Wang, W.; Du, Y.; Jin, Z. L. VLE Measurement and Correlation of N<sub>2</sub>-Ar-CH<sub>4</sub> System at 122.89 K. *Huaxue Gongcheng* **1988**, *16*, 58–63.
- (35) Rozhnov, M. S.; Kozya, V. G.; Zhdanov, V. I. Phase Relationships in C<sub>1</sub>-C<sub>3</sub> Hydrocarbons and Nitrogen 2-Component Systems. *Khim. Prom-st. (Moscow)* **1988**, 674–675.
- (36) Jin, Z.; Liu, K.; Sheng, W. Vapor-Liquid Equilibrium in Binary and Ternary Mixtures of Nitrogen, Argon, and Methane. *J. Chem. Eng. Data* **1993**, *38*, 353–355, DOI: 10.1021/je00011a004.
- (37) Parrish, W. R.; Hiza, M. J. Liquid-Vapor Equilibria in the Nitrogen + Methane System between 95 and 120 K. *Adv. Cryog. Eng.* **1995**, *19*, 300–308, DOI: 10.1007/978-1-4613-9847-9\_37.
- (38) Janisch, J.; Raabe, G.; Kohler, J. Vapor-Liquid Equilibria and Saturated Liquid Densities in Binary Mixtures of Nitrogen, Methane, and Ethane and Their Correlation Using the VTPR and PSRK GCEOS. *J. Chem. Eng. Data* **2007**, *52*, 1897–1903, DOI: 10.1021/je700210n.
- (39) Han, X. H. H.; Zhang, Y. J. J.; Gao, Z. J.; Xu, Y. J.; Wang, Q.; Chen, G. M. Vapor-Liquid Equilibrium for the Mixture Nitrogen (N<sub>2</sub>) + Methane (CH<sub>4</sub>) in the Temperature Range of (110 to 125) K. *J. Chem. Eng. Data* **2012**, *57*, 1621–1626, DOI: 10.1021/je201299u.

- (40) Ellington, R. T.; Eakin, B. E.; Parent, J. D.; Gami, D. C.; Bloomer, O. T. Vapor-Liquid Phase Equilibria in the Binary Systems of Methane, Ethane and Nitrogen. Thermodynamic Transport Properties of Gases, Liquids, Solids, Symposium. Lafayette: Indiana, 1959.
- (41) Stryjek, R.; Chappellear, P. S.; Kobayashi, R. Low-Temperature Vapor-Liquid Equilibria of Nitrogen + Ethane System. *J. Chem. Eng. Data* **1974**, *19*, 340–343, DOI: 10.1021/je60063a024.
- (42) Grauso, L.; Fredenslund, A.; Mollerup, J. M. Vapour-Liquid Equilibrium Data for the Systems  $C_2H_6 + N_2$ ,  $C_2H_4 + N_2$ ,  $C_3H_8 + N_2$ , and  $C_3H_6 + N_2$ . *Fluid Phase Equilib.* **1977**, *1*, 13–26, DOI: 10.1016/0378-3812(77)80022-8.
- (43) Gupta, M. K.; Gardner, G. C.; Hegarty, M. J.; Kidnay, A. J. Liquid-Vapor Equilibria for the  $N_2 + CH_4 + C_2H_6$  System From 260 to 280 K. *J. Chem. Eng. Data* **1980**, *25*, 313–318, DOI: 10.1021/je60087a016.
- (44) Kremer, H.; Knapp, H. Three-Phase Conditions are Predictable. *Hydrocarbon Process.* **1983**, *62*, 79–83.
- (45) Zeck, S.; Knapp, H. Vapor-Liquid and Vapor-Liquid-Liquid Phase Equilibria for Binary and Ternary Systems of Nitrogen, Ethane and Methanol: Experiment and Data Reduction. *Fluid Phase Equilib.* **1986**, *25*, 303–322, DOI: 10.1016/0378-3812(86)80006-1.
- (46) Brown, T. S.; Sloan, E. D.; Kidnay, A. J. Vapor-Liquid Equilibria in the Nitrogen + Carbon Dioxide + Ethane System. *Fluid Phase Equilib.* **1989**, *51*, 299–313, DOI: 10.1016/0378-3812(89)80372-3.
- (47) Zhang, Z.; Guo, L.; Yang, X.; Knapp, H. Vapor and Liquid Equilibrium for Nitrogen - Ethane - Carbon Dioxide Ternary System. *Huagong Xuebao* **1999**, *50*, 392–398.
- (48) Raabe, G.; Janisch, J.; Koehler, J. Experimental Studies of Phase Equilibria in Mixtures Relevant for the Description of Natural Gases. *Fluid Phase Equilib.* **2001**, *185*, 199–208, DOI: 10.1016/s0378-3812(01)00470-8.
- (49) Guedes, H. J. R.; Zollweg, J. A. Thermodynamics of Liquid (Nitrogen + Ethane). *J. Chem. Thermodyn.* **2002**, *34*, 669–678, DOI: 10.1006/jcht.2001.0936.
- (50) Raabe, G.; Kohler, J. Phase Equilibria in the System Nitrogen-Ethane and Their Prediction Using Cubic Equations of State with Different Types of Mixing Rules. *Fluid Phase Equilib.* **2004**, *222-223*, 3–9, DOI: 10.1016/j.fluid.2004.06.001.
- (51) Bolshakov, P. E.; Linshits, L. R. Phase Equilibria in Systems Liquid - Gas at High Pressures. *Trudy GIAP* **1954**, 18–27.
- (52) Schindler, D. L.; Swift, G. W.; Kurata, F. More Low Temperature V-L Design Data. *Hydrocarbon Process.* **1966**, *45*, 205–210.
- (53) Cannon, W.; Robson, J.; English, W. *Liquid Propellant Gas Absorption Study*; Douglas Missile Space Syst. Div. Astropower Lab.: Newport Beach: Calif., 1968; DAC-60510-F2.
- (54) Yorizane, M.; Sadamoto, S.; Yoshimura, S.; Masuoka, H.; Shiki, N.; Kimura, T.; Toyama, A. Vapor-Liquid Equilibrium at Low Temperature Nitrogen + Propylene and Carbon Monoxide + Methane Systems. *Kagaku Kogaku* **1968**, *32*, 257–264.
- (55) Hudziak, J. A.; Kahvand, H.; Yasale, M.; Leipziger, S. Dew Point Measurements for Nitrogen + Propane and Nitrogen + Butane Mixtures. *J. Chem. Eng. Data* **1984**, *29*, 296–301, DOI: 10.1021/je00037a022.

- (56) Poon, D. P. L.; Lu, B. C.-Y. Phase Equilibria for Systems Containing Nitrogen, Methane, and Propane. *Adv. Cryog. Eng.* **1995**, *19*, 292–299, DOI: 10.1007/978-1-4613-9847-9\_36.
- (57) Yucelen, B.; Kidnay, A. J. Vapor-Liquid Equilibria in the Nitrogen + Carbon Dioxide + Propane System from 240 to 330 K at Pressures to 15 MPa. *J. Chem. Eng. Data* **1999**, *44*, 926–931, DOI: 10.1021/je980321e.
- (58) Sauer, R. N. Vapor-Liquid Equilibria in the Nitrogen-Methane-*n*-Butane System. M.Sc. thesis, University of Texas, 1959.
- (59) Roberts, L. R.; McKetta, J. J. Vapor-Liquid Equilibrium in the *n*-Butane-Nitrogen System. *AIChE J.* **1961**, *7*, 173–174, DOI: 10.1002/aic.690070137.
- (60) Roberts, L. R.; McKetta, J. J. Vapor-Liquid Equilibrium in the *n*-Butane-Methane-Nitrogen System. *J. Chem. Eng. Data* **1963**, *8*, 161–163, DOI: 10.1021/je60017a001.
- (61) Lehigh, W. R.; McKetta, J. J. Vapor-Liquid Equilibrium in the Ethane-*n*-Butane-Nitrogen System. *J. Chem. Eng. Data* **1966**, *11*, 180–182, DOI: 10.1021/je60029a015.
- (62) Steinbach, H. G.; Steinbrecher, M. Solubility of Nitrogen in C<sub>4</sub> Liquefied Gases. *Chem. Tech. (Leipzig)* **1966**, *18*, 633.
- (63) Brown, T. S.; Niesen, V. G.; Sloan, E. D.; Kinday, A. J. Vapor-Liquid Equilibria for the Binary Systems of Nitrogen, Carbon Dioxide, and *n*-Butane at Temperatures from 220 to 344 K. *Fluid Phase Equilib.* **1989**, *53*, 7–14, DOI: 10.1016/0378-3812(89)80067-6.
- (64) Malewski, M. K. F.; Sandler, S. I. High-Pressure Vapor-Liquid Equilibria of the Binary Mixtures Nitrogen + *n*-Butane and Argon + *n*-Butane. *J. Chem. Eng. Data* **1989**, *34*, 424–426, DOI: 10.1021/je00058a015.
- (65) Shibata, S. K.; Sandler, S. I. High-Pressure Vapor-Liquid Equilibria Involving Mixtures of Nitrogen, Carbon Dioxide, and *n*-Butane. *J. Chem. Eng. Data* **1989**, *34*, 291–298, DOI: 10.1021/je00057a011.
- (66) Brown, T. S.; Sloan, E. D.; Kidnay, A. J. Vapor-Liquid Equilibria for the Ternary System N<sub>2</sub> + CO<sub>2</sub> + *n*-C<sub>4</sub>H<sub>10</sub> at 250 and 270 K. *Int. J. Thermophys.* **1994**, *15*, 1211–1219, DOI: 10.1007/bf01458829.
- (67) Kurata, F.; Swift, G. W. *Experimental Measurements of Vapor-Liquid Equilibrium for the Ethane-Carbon Dioxide and Nitrogen-*n*-Pentane Binary Systems*; Research Report RR-5: Tulsa, OK, 1971; Assoc.
- (68) Preston, G. T.; Prausnitz, J. M. Solubilities of *n*-Pentane and 1,3-Butadiene in Liquid Nitrogen. *J. Chem. Eng. Data* **1972**, *17*, 465–465, DOI: 10.1021/je60055a014.
- (69) Kalra, H.; Robinson, D. B.; Besserer, G. J. The Equilibrium Phase Properties of the Nitrogen + *n*-Pentane System. *J. Chem. Eng. Data* **1977**, *22*, 215–218, DOI: 10.1021/je60073a023.
- (70) Silva-Oliver, G.; Eliosa-Jimenez, G.; Garcia-Sanchez, F.; Avendano-Gomez, J. R. High-Pressure Vapor Liquid Equilibria in the Nitrogen *n*-Pentane System. *Fluid Phase Equilib.* **2006**, *250*, 37–48, DOI: 10.1016/j.fluid.2006.09.018.
- (71) Poston, R. S.; McKetta, J. J. Vapor-Liquid Equilibrium in the *n*-Hexane - Nitrogen System. *J. Chem. Eng. Data* **1966**, *11*, 364–365, DOI: 10.1021/je60030a022.
- (72) Baranovich, Z. N.; Smirnova, A. M. Solubility of Nitrogen in *n*-Hexane and *n*-

- Octane at Low Temperatures. *Zh. Prikl. Khim.* **1972**, *45*, 2776–2778.
- (73) Hesse, P. J.; Battino, R.; Scharlin, P.; Wilhelm, E. Solubility of Gases in Liquids. 20. Solubility of He, Ne, Ar, Kr, N<sub>2</sub>, O<sub>2</sub>, CH<sub>4</sub>, CF<sub>4</sub>, and SF<sub>6</sub> in *n*-Alkanes *n*-C<sub>l</sub>H<sub>2l+2</sub> ( $6 \leq l \leq 16$ ) at 298.15 K. *J. Chem. Eng. Data* **1996**, *41*, 195–201, DOI: 10.1021/je9502455.
- (74) Eliosa-Jimenez, G.; Silva-Oliver, G.; Garcia-Sanchez, F.; de Ita de la Torre, A. High-Pressure Vapor-Liquid Equilibria in the Nitrogen + *n*-Hexane System. *J. Chem. Eng. Data* **2007**, *52*, 395–404, DOI: 10.1021/je060341d.
- (75) Jabloniec, A.; Horstmann, S.; Gmehling, J. Experimental Determination and Calculation of Gas Solubility Data for Nitrogen in Different Solvents. *Ind. Eng. Chem. Res.* **2007**, *46*, 4654–4659, DOI: 10.1021/ie061258m.
- (76) Akers, W. W.; Kehn, D. M.; Kilgore, C. H. Volumetric and Phase Behaviour of Nitrogen-Hydrocarbon Systems Nitrogen-*n*-Heptane System. *Ind. Eng. Chem.* **1954**, *46*, 2536–2539, DOI: 10.1021/ie50540a040.
- (77) Peter, S.; Eicke, H. F. Phase Equilibria in the Systems Nitrogen + *n*-Heptane, Nitrogen + 2,2,4-Trimethylpentane, and Nitrogen + Methylcyclohexane at High Pressures and Temperatures. *Ber. Bunsen-Ges. Phys. Chem.* **1970**, *74*, 190–194.
- (78) Brunner, G.; Peter, S.; Wenzel, H. Phase Equilibrium in the Systems *n*-Heptane - Nitrogen; Methylcyclohexane - Nitrogen and *n*-Heptane - Methylcyclohexane - Nitrogen at High Pressures. *Chem. Eng. J.* **1974**, *7*, 99–104, DOI: 10.1016/0300-9467(74)85002-1.
- (79) Figuiere, P.; Hom, J. F.; Laugier, S.; Renon, H.; Richon, D.; Szwarc, H. Vapor-Liquid Equilibria up to 40,000 kPa and 400°C: A New Static Method. *AIChE J.* **1980**, *26*, 872.
- (80) Legret, D.; Richon, D.; Renon, H. Vapor Liquid Equilibria up to 100 MPa: a New Apparatus. *AIChE J.* **1981**, *27*, 203–207, DOI: 10.1002/aic.690270205.
- (81) Llave, F. M.; Chung, T. H. Vapor-Liquid Equilibria of Nitrogen-Hydrocarbon Systems at Elevated Pressures. *J. Chem. Eng. Data* **1988**, *33*, 123–128, DOI: 10.1021/je00052a019.
- (82) Waeterling, U.; Zheng, D.; Knapp, H. Vapor-Liquid Equilibria at High Temperatures and Pressures in Binary Mixtures Containing Hydrogen, Methane, and Carbon Dioxide with High Boiling Hydrocarbons: Experimental Equipment and Results. *Chem. Eng. Process.* **1991**, *29*, 155–164.
- (83) Schlichting, H.; Langhorst, R.; Knapp, H. Saturation of High Pressure Gases with Low Volatile Solvents: Experiments and Correlation. *Fluid Phase Equilib.* **1993**, *84*, 143–163, DOI: 10.1016/0378-3812(93)85121-2.
- (84) Garcia-Sanchez, F.; Eliosa-Jimenez, G.; Silva-Oliver, G.; Godinez-Silva, A. High-Pressure (Vapor + Liquid) Equilibria in the (Nitrogen + *n*-Heptane) System. *J. Chem. Thermodyn.* **2007**, *39*, 893–905, DOI: 10.1016/j.jct.2006.11.007.
- (85) Daridon, J. L.; Lagourette, B.; Xans, P. Thermodynamic Properties of Liquid Mixtures Containing Gas Under Pressure Based on Ultrasonic Measurements. *Fluid Phase Equilib.* **1994**, *100*, 269–282, DOI: 10.1016/0378-3812(94)80014-6.
- (86) Eliosa-Jimenez, G.; Garcia-Sanchez, F.; Silva-Oliver, G.; Macias-Salinas, R. Vapor Liquid Equilibrium Data for the Nitrogen + *n*-Octane System from (344.5 to 543.5)K and at Pressures up to 50 MPa. *Fluid Phase Equilib.* **2009**, *282*, 3–10, DOI: 10.1016/j.fluid.2009.04.015.

- (87) Silva-Oliver, G.; Eliosa-Jimenez, G.; Garcia-Sanchez, F.; Avendano-Gomez, J. R. High-Pressure Vapor-Liquid Equilibria in the Nitrogen *n*-Nonane System. *J. Supercrit. Fluids* **2007**, *42*, 36–47.
- (88) Prausnitz, J. M.; Benson, P. R. Solubility of Liquids in Compressed Hydrogen, Nitrogen and Carbon Dioxide. *AIChE J.* **1959**, *5*, 161–164.
- (89) Azarnoosh, A.; McKetta, J. J. Nitrogen - *n*-Decane System in Two-Phase Region. *J. Chem. Eng. Data* **1963**, *8*, 494–496, DOI: 10.1021/je60019a005.
- (90) D’Avila, S. G.; Kaul, B. K.; Prausnitz, J. M. Solubilities of Heavy Hydrocarbons in Compressed Methane and Nitrogen. *J. Chem. Eng. Data* **1976**, *21*, 488–491, DOI: 10.1021/je60071a017.
- (91) Pearce, D. L.; Peters, C. J.; de Swaan Arons, J. Measurement of the Gas Phase Solubility of Decane in Nitrogen. *Fluid Phase Equilib.* **1993**, *89*, 335–343, DOI: 10.1016/0378-3812(93)85092-z.
- (92) Tong, J.; Gao, W.; Robinson, R.; Gasem, K. A. M. Solubilities of Nitrogen in Heavy Normal Paraffins from 323 to 423 K at Pressures to 18.0 MPa. *J. Chem. Eng. Data* **1999**, *44*, 784–787, DOI: 10.1021/je980279n.
- (93) Garcia-Sanchez, F.; Eliosa-Jimenez, G.; Silva-Oliver, G.; Garcia-Flores, B. E. Vapor-Liquid Equilibrium Data for the Nitrogen + *n*-Decane System from (344 to 563) K and at Pressures up to 50 MPa. *J. Chem. Eng. Data* **2009**, *54*, 1560–1568, DOI: 10.1021/je800881t.
- (94) Gao, W.; Robinson, R.; Gasem, K. A. M. High-Pressure Solubilities of Hydrogen, Nitrogen, and Carbon Monoxide in Dodecane from 344 to 410 K at Pressures to 13.2 MPa. *J. Chem. Eng. Data* **1999**, *44*, 130–132, DOI: 10.1021/je9801664.
- (95) Garcia-Cordova, T.; Justo-Garcia, D. N.; Garcia-Flores, B. E.; Garcia-Sanchez, F. Vapor-Liquid Equilibrium Data for the Nitrogen + Dodecane System at Temperatures from (344 to 593) K and at Pressures up to 60 MPa. *J. Chem. Eng. Data* **2011**, *56*, 1555–1564, DOI: 10.1021/je1012372.
- (96) Sultanov, R. G.; Skripka, V. G.; Namiot, A. Y. Phase Equilibrium of Methane and Nitrogen with High-boiling Hydrocarbons. *Gazov. Delo* **1972**, *10*, 43–46.
- (97) Lin, H. M.; Kim, H.; Chao, K.-C. Gas-Liquid Equilibria in Nitrogen + *n*-Hexadecane Mixtures at Elevated Temperatures and Pressures. *Fluid Phase Equilib.* **1981**, *7*, 181–185, DOI: 10.1016/0378-3812(81)85020-0.
- (98) Rowane, A. J.; Gavaises, M.; McHugh, M. A. Vapor-Liquid Equilibria and Mixture Densities for 2,2,4,4,6,8,8-heptamethylnonane + N<sub>2</sub> and *n*-Hexadecane + N<sub>2</sub> Binary Mixtures up to 535 K and 135 MPa. *Fluid Phase Equilib.* **2020**, *506*, 112378, DOI: 10.1016/j.fluid.2019.112378.
- (99) Robinson, D. B.; Kalra, H.; Krishnan, T. R.; Miranda, R. The Phase Behavior of Selected Hydrocarbon - Non Hydrocarbon Binary Systems: C<sub>2</sub> – H<sub>2</sub>S and N<sub>2</sub> – *i*C<sub>4</sub> Systems. *Proc. Annu. Conv. Gas Process. Assoc.* 1975; pp 25–31.
- (100) Robinson, D. B.; Kalra, H. *The Equilibrium Phase Properties of Selected Binary Systems: n-Heptane-Hydrogen Sulfide, n-Heptane-Carbon Dioxide, i-Butane- Nitrogen*; GPA, 1976; 18.
- (101) Kalra, H.; Ng, H.-J.; Miranda, R. D.; Robinson, D. B. Equilibrium Phase Properties of the Nitrogen-Isobutane System. *J. Chem. Eng. Data* **1978**, *23*, 321–324, DOI: 10.1021/je60079a022.

- (102) Chen, G.; Knapp, H.; Hou, Y. Vapor-Liquid Equilibria for the Nitrogen-Isobutane System. *J. Solution Chem.* **1997**, *26*, 779–790, DOI: 10.1007/bf02767783.
- (103) Krishnan, T. R.; Kalra, H.; Robinson, D. B. The Equilibrium Phase Properties of the Nitrogen-Isopentane System. *J. Chem. Eng. Data* **1977**, *22*, 282–285, DOI: 10.1021/je60074a012.
- (104) Reisig, H.; Schneider, G. M. Fluid-Phase and Crystallization Equilibria of the Binary System Nitrogen + Dimethylpropane between 190 and 300 K and at Pressures up to 200 MPa. *Fluid Phase Equilib.* **1989**, *45*, 103–114, DOI: 10.1016/0378-3812(89)80169-4.
- (105) Hesse, P. J.; Battino, R.; Scharlin, P.; Wilhelm, E. Solubility of Gases in Liquids. 21. Solubility of He, Ne, Ar, Kr, N<sub>2</sub>, O<sub>2</sub>, CH<sub>4</sub>, CF<sub>4</sub>, and SF<sub>6</sub> in 2,2,4-Trimethylpentane at  $T = 298.15$  K. *J. Chem. Thermodyn.* **1999**, *31*, 1175–1181, DOI: 10.1006/jcht.1999.0529.
- (106) Zhang, J. S.; Lee, J. W. Solubility of CO<sub>2</sub>, N<sub>2</sub>, and CO<sub>2</sub> + N<sub>2</sub> Gas Mixtures in Isooctane. *J. Chem. Eng. Data* **2008**, *53*, 1321–1324, DOI: 10.1021/je800053f.
- (107) Marathe, P.; Sandler, S. I. High-Pressure Vapor-Liquid Equilibrium of Some Binary Mixtures of Cyclopentane, Argon, Nitrogen, *n*-Butane, and Neopentane. *J. Chem. Eng. Data* **1991**, *36*, 192–197, DOI: 10.1021/je00002a015.
- (108) Wilhelm, E.; Battino, R. The Solubility of Gases in Liquids: 5 the Solubility of Nitrogen, Oxygen, Carbon Monoxide, and Carbon Dioxide in Cyclohexane at 283 to 313 K. *J. Chem. Thermodyn.* **1973**, *5*, 117–120, DOI: 10.1016/s0021-9614(73)80068-0.
- (109) Vosmanský, J.; Dohnal, V. Gas Solubility Measurements with an Apparatus of the Ben-Naim-Baer Type. *Fluid Phase Equilib.* **1987**, *33*, 137–155, DOI: 10.1016/0378-3812(87)87008-5.
- (110) Shibata, S. K.; Sandler, S. I. High-Pressure Vapor-Liquid Equilibria of Mixtures of Nitrogen, Carbon Dioxide, and Cyclohexane. *J. Chem. Eng. Data* **1989**, *34*, 419–424, DOI: 10.1021/je00058a014.
- (111) Gao, W.; Gasem, K. A. M.; Robinson Jr., R. L. Solubilities of Nitrogen in Selected Naphthenic and Aromatic Hydrocarbons at Temperatures from 344 to 433 K and Pressures to 22.8 MPa. *J. Chem. Eng. Data* **1999**, *44*, 185–189, DOI: 10.1021/je980187y.
- (112) Lebedeva, E. S.; Kashirina, A. S.; Grokholskaya, V. P. Phase Equilibria in Systems Methylcyclohexane + Nitrogen & Coefficient Distribution Methyl derivative of Cyclic Ketone & Alcohol Between Methylcyclohexane & Water. *Trudy GIAP* **1973**, 9–16.
- (113) Robinson, D. B.; Huang, S. S.; Leu, A.-L. *The Equilibrium Phase Properties of Selected Naphthenic Binary Systems: Methylcyclohexane Nitrogen Ethylcyclohexane Hydrogen Sulfide n-Propylcyclohexane Hydrogen Sulfide*; GPA, 1981; 51.
- (114) Laugier, S.; Alali, P.; Valtz, A.; Chareton, A.; Fontalba, F.; Richon, D.; Renon, H. *Vapor-Liquid Equilibria Measurements on the Systems N<sub>2</sub>-n-Propylcyclohexane, CO<sub>2</sub>-n-Propylcyclohexane, CH<sub>4</sub>-n-Propylcyclohexane, CH<sub>4</sub>-n-Propylbenzene, and CO<sub>2</sub>-n-Propylbenzene*; GPA, 1984; 75.
- (115) Richon, D.; Laugier, S.; Renon, H. High-Pressure Vapor-Liquid Equilibrium Data for Binary Mixtures Containing Molecular Nitrogen, Carbon Dioxide, Hydrogen Sulfide and an Aromatic Hydrocarbon or Propylcyclohexane in the Range 313–473

- K. *J. Chem. Eng. Data* **1992**, *37*, 264–268, DOI: 10.1021/je00006a035.
- (116) Liu, X.; Liu, S.; Bai, L.; He, M. Measurement and Correlation of the Solubilities of Oxygen, Nitrogen, and Carbon Dioxide in JP-10. *J. Chem. Eng. Data* **2017**, *62*, 3998–4005, DOI: 10.1021/acs.jced.7b00692.
- (117) Lebedeva, E.; Tyurikova, N.; Grokholskaya, V. *Trudy GIAP* **1973**, *20*, 27.
- (118) Lewis, W. K.; Luke, C. D. Vapor-Liquid Equilibria of Hydrocarbons at High Pressure. *Ind. Eng. Chem.* **1933**, *25*, 725–727.
- (119) Miller, P.; Dodge, B. F. The System Benzene-Nitrogen. Liquid-Vapor Phase Equilibria at Elevated Pressures. *Ind. Eng. Chem.* **1940**, *32*, 434–438.
- (120) Gamburg, D. Y. Volume Relations in Dilute Gaseous Solutions as a Function of the Pressure. *Zh. Fiz. Khim.* **1952**, *26*, 1122.
- (121) Coan, C. R.; King, A. D. Second Cross Virial Coefficients of Benzene + Gas Mixtures from High Pressure Solubility Measurements a Comparison with Gas Chromatographic Values. *J. Chromatogr.* **1969**, *44*, 429.
- (122) de Leeuw, V. V.; Poot, W.; de Loos, T. W.; de Swaan Arons, J. High Pressure Phase Equilibria of the Binary Systems Nitrogen + Benzene, Nitrogen + *p*-Xylene and Nitrogen + Naphthalene. *Fluid Phase Equilib.* **1989**, *49*, 75–101, DOI: 10.1016/0378-3812(89)80007-x.
- (123) Tsuji, T.; Ohya, K.; Lai, A. J. X.; Manaf, N. B. A.; Hoshina, T.-a.; Oba, S. Gas Solubilities of Nitrogen or Oxygen in Benzene, Divinylbenzene, Styrene and of an Equimolar (N<sub>2</sub>:O<sub>2</sub>) Mixture in Styrene at (293–313) K. *Fluid Phase Equilib.* **2019**, *492*, 34–40, DOI: 10.1016/j.fluid.2019.03.016.
- (124) Lai, A. J. X.; Tsuji, T.; Tan, L. S.; Bharath, R.; Hoshina, T.-a.; Funazukuri, T. Argon Gas Solubility in Styrene and Nitrogen, Oxygen and Argon Gas Solubilities in Methyl Methacrylate at (293 to 313) K and at Pressures up to 3.8 MPa. *J. Solution Chem.* **2021**, *50*, 1008–1026, DOI: 10.1007/s10953-021-01101-7.
- (125) Laugier, S.; Legret, D.; Desteve, J.; Richon, D.; Renon, H. *Vapor-Liquid Equilibria Measurements on the Systems: N<sub>2</sub>-Toluene, N<sub>2</sub>-*m*-Xylene, and N<sub>2</sub>-Mesitylene*; Gas Processors Association Research Report, 1982; RR-59.
- (126) Lin, H. M.; Lee, M. J.; Lee, R. J. Phase Equilibria of Toluene in Mixtures with Helium or Nitrogen at High Temperatures. *J. Chem. Eng. Data* **1995**, *40*, 653–656, DOI: 10.1021/je00019a027.
- (127) Bian, B.; Wang, Y.; Shi, J. Solubility of Hydrogen Chloride and Chloromethane in 1,2,4-Trimethylbenzene. *Huagong Xuebao* **1987**, 385–393.
- (128) Chareton, A.; Valtz, A.; Lafeuil, C.; Laugier, S.; Richon, D.; Renon, H. *Vapor-Liquid Equilibria Measurements on the Systems Methane-Methylcyclohexane, Nitrogen-*n*-Propylbenzene, Hydrogen Sulfide-*n*-Propylbenzene, Propane-Toluene, Propane-*m*-Xylene and Propane-Methylcyclohexane*; GPA, 1986; 101.
- (129) Renon, H.; Laugier, S.; Schwartzentruber, J.; Richon, D. New Determinations of High Pressure vapor-liquid Equilibria in Binary Systems Containing *n*-Propylbenzene with Nitrogen or Carbon Dioxide Consistent with the Prausnitz-Keeler Test. *Fluid Phase Equilib.* **1989**, *51*, 285–298, DOI: 10.1016/0378-3812(89)80371-1.
- (130) Lin, H. M.; Lee, M. J.; Lee, R. J. High-Temperature Phase Equilibria for Asymmetric Mixtures of Helium + *m*-Xylene

and Nitrogen *m*-Xylene. *Ind. Eng. Chem. Res.* **1995**, *34*, 4524–4530, DOI: 10.1021/ie00039a046.

- (131) Lin, H. M.; Kim, H.; Chao, K.-C. Vapor-Liquid Equilibrium in Nitrogen + 1-Methylnaphthalene Mixtures at Elevated Temperatures and Pressures. *Fluid Phase Equilib.* **1983**, *10*, 73–76, DOI: 10.1016/0378-3812(83)80005-3.
- (132) Kim, H.; Wang, W.; Lin, H. M.; Chao, K. C. Vapor-Liquid Equilibriums in Binary Mixtures of Nitrogen + Tetralin and Nitrogen + *m*-Cresol. *J. Chem. Eng. Data* **1983**, *28*, 216–218, DOI: 10.1021/je00032a028.
- (133) Sauer, E.; Stavrou, M.; Gross, J. Comparison between a Homo- and a Heterosegmented Group Contribution Approach Based on the Perturbed-Chain Polar Statistical Associating Fluid Theory Equation of State. *Ind. Eng. Chem. Res.* **2014**, *53*, 14854–14864, DOI: 10.1021/ie502203w.
- (134) Bell, I. H.; Deiters, U. K. Superancillary Equations for Nonpolar Pure Fluids Modeled with the PC-SAFT Equation of State. *Ind. Eng. Chem. Res.* **2023**, *62*, 1958–1967, DOI: 10.1021/acs.iecr.2c02916.
- (135) Lemmon, E. W.; Span, R. Short Fundamental Equations of State for 20 Industrial Fluids. *J. Chem. Eng. Data* **2006**, *51*, 785–850, DOI: 10.1021/je050186n.
- (136) Bell, I. H.; Deiters, U. K.; Jäger, A. Algorithm to Identify Vapor–Liquid–Liquid Equilibria of Binary Mixtures from Vapor–Liquid Equilibria. *Ind. Eng. Chem. Res.* **2022**, *61*, 2592–2599, DOI: 10.1021/acs.iecr.1c04703.
- (137) Rokni, H. B.; Gupta, A.; Moore, J. D.; McHugh, M. A.; Bamgbade, B. A.; Gavaises, M. Purely Predictive Method for Density, Compressibility, and Expansivity for Hydrocarbon Mixtures and

Diesel and Jet Fuels up to High Temperatures and Pressures. *Fuel* **2019**, *236*, 1377–1390, DOI: 10.1016/j.fuel.2018.09.041.

# TOC Graphic

